Stability of two-layer Newtonian plane Couette flow past a deformable solid layer

V. Shankar[a] and Lalit Kumar
Department of Chemical Engineering, Indian Institute of Technology, Kanpur 208 016, India

(Received 7 April 2004; accepted 17 August 2004; published online 2 November 2004)

The linear stability of two-layer plane Couette flow of Newtonian fluids (designated by labels *A* and *B*) of thicknesses $(1-\beta)R$ and βR, and viscosities μ_a and μ_b past a soft, deformable linear viscoelastic solid of thickness *HR*, shear modulus *G*, and viscosity η_w is determined using a combination of low wavenumber asymptotic analysis and a numerical method. There are two qualitatively different interfacial modes in this system, viz., the two-fluid interfacial mode due to viscosity stratification ["mode 1;" C. S. Yih "Instability due to viscosity stratification," J. Fluid Mech. **27**, 337 (1967)], and the fluid–solid interfacial mode ["mode 2;" Kumaran, Fredrickson, and Pincus, "Flow induced instability of the interface between a fluid and a gel at low Reynolds number," J. Phys II **4**, 893 (1994)]. The respective effects of solid layer deformability and fluid viscosity stratification on mode 1 and mode 2 are analyzed in detail using both asymptotic and numerical methods. Results of our low wavenumber asymptotic analysis show that the deformability of the solid layer has a dramatic effect on the interfacial instability (mode 1) between the two Newtonian fluids: When the more viscous fluid is of smaller thickness (an unstable configuration for the two-fluid mode 1 instability), the solid layer could completely *stabilize* the two-fluid interfacial instability, when the nondimensional elasticity parameter $\Gamma = V\mu_b/(GR)$ increases beyond a critical value. Here *V* is the dimensional velocity of the top moving plate. When the more viscous fluid is of larger thickness compared to the less viscous fluid (a stable configuration in rigid channels), it is shown that the solid layer could *destabilize* or stabilize the two-fluid interfacial mode, depending on the solid layer thickness *H*. Numerical results at finite values of wavenumber *k* reveal that the stabilization of the two-fluid interfacial mode predicted by the low wavenumber analysis extends to moderate values of *k*. For high values of *k*, the perturbations are localized near the two-fluid interface. Increase in Γ therefore does not have any effect on the high *k* unstable modes, which are stabilized by the presence of nonzero interfacial tension in the two-fluid interface. When Γ is further increased, the interfacial mode between fluid *B* and the solid layer becomes unstable. It is demonstrated here that the parameters Γ (representing the shear modulus of the solid), solid layer thickness *H*, and the solid layer viscosity η_w can be chosen such that both the interfacial modes are stabilized at all wavenumbers, for a fixed top plate velocity. © *2004 American Institute of Physics*. [DOI: 10.1063/1.1808772]

I. INTRODUCTION

The flow of fluids past soft, deformable solid surfaces occurs in a wide variety of settings such as in biological systems where the flow of blood and other fluids occurs in deformable tubes, in biotechnological applications such as membrane bioreactors, and more recently, in microfluidic devices where soft elastomers are used in the fabrication of microchannels.[1,2] A clear understanding of fluid flow past soft solid surfaces, and the way in which the solid interacts with the flow, will help in the accurate design and development of these applications. The shear modulus of soft solids is relatively low (~10 kPa–1 MPa), and thus such soft solids can be deformed by moderate fluid stresses. The dynamics of fluid flow past soft solids is very different from that of flow past rigid surfaces due to the deformability of the solid surface, which couples the dynamics of the fluid with the deformation of the solid. In particular, this coupling could lead to interfacial instabilities between the fluid and the solid, as first theoretically predicted by Kumaran *et al.*,[3] and experimentally demonstrated by Kumaran and Muralikrishnan.[4,5] An interesting feature concerning these instabilities is that they can occur even in the creeping flow limit, in the absence of fluid and solid inertia. Subsequent theoretical studies[6–9] have shown that qualitatively new instabilities exist in flow past deformable solid surfaces even in the high Reynolds number regime, and these instabilities are not continuation of existing instabilities in flow past rigid solid surfaces.

The study of interfacial instabilities between *two fluids* undergoing shear flow has also been an area of extensive research, beginning from the pioneering work of Yih.[10] These studies are motivated in part by their relevance to polymer processing applications such as multilayer extrusion, where an accurate understanding of stable and unstable processing conditions can help in preventing interfacial in-

[a]Author to whom correspondence should be addressed. Electronic mail: vshankar@iitk.ac.in

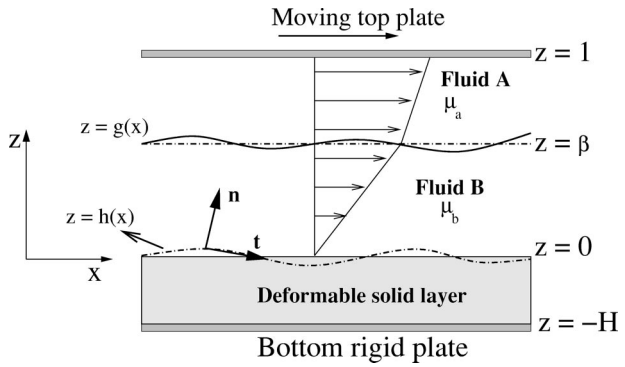

FIG. 1. Schematic diagram showing the configuration and (nondimensional) coordinate system considered in this paper: two Newtonian fluids of viscosities μ_a and μ_b flowing past a deformable solid layer.

stabilities that are detrimental to product quality. Subsequent to the study of Yih, a large number of studies (for an extensive review, see Joseph and Renardy[11]) have focused on the theoretical understanding of interfacial instabilities in two-layer and multilayer flows of Newtonian and viscoelastic fluids. These studies have clearly identified the parameter regimes in which interfacial instabilities occur, and have elucidated the physical mechanisms that underlie such instabilities.

In this paper, we consider the stability of the three layer configuration consisting of a *two-layer* flow of Newtonian fluids of different viscosities undergoing plane Couette flow past a soft, deformable solid layer (see Fig. 1). Such a configuration might be relevant in polymer processing, where one might envisage the use of soft solid layer coatings to manipulate and control the interfacial instabilities. Indeed, there exists an extensive body of literature (see, for example, Ref. 12) which has studied the stability of *single-layer* Newtonian flow past compliant walls, in order to explore the possibility of delaying the onset of instabilities by wall deformability, and thereby achieve drag reduction at high Reynolds numbers. These studies have shown, however, that while deformable walls may delay the boundary layer instability past rigid surfaces, they usually induce additional modes of instabilities that arise due to the deformable nature of the wall. In this study, we explore the possibility of the use of soft solid layers to control and manipulate the interfacial instabilities in two-layer flows of Newtonian fluids, in the low (but finite) Reynolds number regime. If soft solid coatings can stabilize the interfacial instabilities, then they could potentially be used to prevent such instabilities in polymer processing applications. While these applications often involve fluids that are viscoelastic in nature, and hence can exhibit additional instabilities due to normal stress differences,[13,14] it is instructive to understand the effect of the solid layer on two-layer flow of Newtonian fluids with viscosity stratification, which is the goal of the present study. In the remainder of this Introduction, relevant previous studies are briefly reviewed, and the context and motivation for the present work is placed in perspective.

Yih[10] first studied the stability of two-layer plane Couette flow of two Newtonian fluids of different viscosities using a long-wave asymptotic analysis and showed that the interface is stable in the absence of fluid inertia. However, even in the presence of a vanishingly small Reynolds number, the interface becomes unstable in the long-wave limit due to viscosity stratification when the thickness of the more viscous fluid is smaller than the thickness of the less viscous fluid. The interface is stable when the thickness of the more viscous fluid is larger than that of the less viscous fluid. It is important to note that the instability of the two-layer system is independent of whether the more viscous fluid is placed adjacent to the stationary plate or the moving plate. Hooper and Boyd[15] considered the interface between two fluids undergoing semi-infinite Couette flow, and showed using an asymptotic analysis that the interface is unstable to short waves. This result applies to any two-layer parallel shear flow because for very short waves, the perturbations are localized near the two-fluid interface. However, the presence of a sufficiently strong nonzero interfacial tension will stabilize this short-wave instability. An approximate "rule of thumb"[11] for a stable arrangement of two-layer plane Couette flow is therefore to place the less viscous fluid in a thin layer (thus stabilizing long waves) and to have sufficiently strong interfacial tension (to stabilize short waves). A number of subsequent studies have analyzed a variety of multilayer shearing flows, and these have been reviewed extensively by Joseph and Renardy.[11] Charru and Hinch[16] used a detailed analysis to understand the physical mechanism that drives the two-fluid instability. They demonstrated *how* the first correction to the velocity field (of the long-wave asymptotic analysis) in the two fluids can set up a flow in such a manner that the fluctuations of the two-fluid interface can be amplified or suppressed under appropriate conditions that result from Yih's analysis.

Kumaran *et al.*[3] studied the stability of the plane Couette flow of a Newtonian fluid of viscosity μ past a deformable wall of finite thickness, which was modeled as an incompressible linear viscoelastic solid of shear modulus G fixed to a rigid substrate. In contrast to the case of two-layer Couette flow of two Newtonian fluids, their analysis showed that the flow is unstable in the absence of fluid and solid inertia ($\mathrm{Re}=0$), and the time dependence entered through the tangential velocity condition at the interface, which coupled the base flow to interfacial perturbations. Their characteristic equation determining the stability of the system was quadratic, and one of the roots becomes unstable when $\Gamma = V\mu/(GR)$ is greater than a certain critical value. The physical mechanism driving this instability was interpreted in terms of a transfer of energy from the mean flow to fluctuations through the deformation work done by the mean flow at the interface. Recently, Gkanis and Kumar,[17] who studied the stability of plane Couette flow past a neo-Hookean solid, have interpreted the instability mechanism in terms of phase relationships between velocity and interfacial perturbations. At the critical conditions, they have shown that the mean flow tends to amplify horizontal perturbations to the interface location, while horizontal velocity perturbations in the fluid tend to suppress them. A similar instability for viscoelastic plane Couette flow past a deformable wall has been predicted by Shankar and Kumar.[18] The study of Srivatsan

and Kumaran[19] has used a numerical procedure and showed that the instability predicted at Re=0 (Ref. 3) extends to finite and large Re. Importantly, these studies have shown that the instability of plane Couette flow past a deformable solid is a finite wavenumber instability, and is stable for perturbations with very large and very small wavelengths. This feature is qualitatively different from the interfacial mode between two Newtonian fluids, which can be unstable at very large wavelengths and very small wavelengths (in the absence of interfacial tension).

For the three-layer configuration under consideration in this study, there are two qualitatively different interfacial modes, viz., the fluid–fluid interfacial mode and the fluid–solid interfacial mode, and both can be unstable when Re $\neq 0$ due to qualitatively different mechanisms discussed above. In this paper, we are interested in studying how these two qualitatively different interfacial modes interact, and the consequences this interaction has on the stability of the two modes. The early study of Li[20] which analyzed the stability of three-layer Newtonian flow with viscosity stratification, had shown that the presence of the second interface rendered the flow unstable even in the creeping flow limit, due to a resonance between the two interfacial modes. This early analysis shows that even in the case of three Newtonian fluids, new phenomena emerge due to the interaction of the two interfacial perturbations. A recent work by one of the authors[21] has analyzed the stability of two-layer viscoelastic plane Couette flow past a deformable solid layer in the creeping flow limit (where fluid and solid layer inertia is neglected) with the fluids having *matched* viscosities. This study shows that it is possible to stabilize the two-fluid instability due to *elasticity* stratification in viscoelastic fluids by the solid layer. This result further provides the motivation to analyze the present configuration of two-layer Newtonian Couette flow past a deformable solid layer, in the presence of finite fluid and solid inertia, and with viscosity stratification.

The rest of this paper is structured as follows: The governing equations, base state, and the linearized stability equations are presented in Sec. II. In Sec. III, we outline the low wavenumber asymptotic analysis for the present three-layer configuration and discuss the important results from this analysis. In Sec. IV A, we briefly discuss the numerical method used to study finite wavenumber perturbations, and in Sec. IV B we provide representative results for the complex wavespeed as a function of the wavenumber, and neutral stability diagrams in appropriate parameter space. The salient results of this work are summarized in Sec. V.

II. PROBLEM FORMULATION

A. Governing equations

The system under consideration (Fig. 1) consists of a linear viscoelastic solid of thickness HR, shear modulus G, and viscosity η_w fixed onto a rigid surface at $z^*=-HR$, a layer of Newtonian fluid (fluid B) of thickness βR in the region $0<z^*<\beta R$ with viscosity μ_b, and another Newtonian fluid (fluid A) of thickness $(1-\beta)R$ in the region $\beta R<z^*<R$ with viscosity μ_a. We have assumed that the densities of the two fluids are equal ($\rho_a=\rho_b=\rho$), in order to exclusively focus on the instability of the two-fluid interface due to viscosity stratification. In what follows, we indicate dimensional variables with a superscript *, and nondimensional variables without any superscript. Fluid A is bounded at $z^*=R$ by a rigid wall which moves at a constant velocity V in the x direction relative to the deformable solid layer. It is useful to nondimensionalize various physical quantities at the outset, and the following scales are used for this purpose: R for lengths and displacements, V for velocities, R/V for time, and $\mu_b V/R$ for stresses and pressure. H, therefore, is the nondimensional thickness of the solid layer, while $(1-\beta)$ and β are, respectively, the nondimensional thickness of fluids A and B.

The nondimensional governing equations in the two fluids are, respectively, the Navier–Stokes continuity and momentum equations:

$$\partial_i v_i^\alpha = 0, \tag{1}$$

$$\mathrm{Re}[\partial_t v_i^\alpha + v_j^\alpha \partial_j v_i^\alpha] = -\partial_i p^\alpha + \mu_r^\alpha \partial_j^2 v_i^\alpha. \tag{2}$$

Here, v_i^α is the velocity field in fluid $\alpha(\alpha=a,b)$, $\partial_t \equiv (\partial/\partial t)$, $\partial_i \equiv (\partial/\partial x_i)$ and the indices i,j take the values x,z, Re $=RV\rho/\mu_b$ is the Reynolds number based on the viscosity of fluid B, and $\mu_r^a \equiv \mu_r = \mu_a/\mu_b$, $\mu_r^b = \mu_b/\mu_b = 1$ are the viscosity ratios. The total stress tensor T_{ij}^α in the two fluids is given by

$$T_{ij}^\alpha = -p^\alpha \delta_{ij} + \tau_{ij}^\alpha, \tag{3}$$

$$\tau_{ij}^\alpha = \mu_r^\alpha (\partial_i v_j^\alpha + \partial_j v_i^\alpha), \tag{4}$$

where τ_{ij}^α is the deviatoric stress tensor in fluid α and p^α is the pressure in fluid α. No-slip boundary conditions are appropriate for fluid A at $z=1$:

$$v_x^a = 1, \quad v_z^a = 0, \tag{5}$$

while the boundary conditions at the interface between the two fluids and the interface between the fluid B and the solid layer are discussed below.

The deformable solid layer is modeled as an incompressible linear viscoelastic solid, similar to that used in the previous studies in this area (see, for example, Refs. 3, 6–8, and 19). The dynamics of the solid layer is described by a displacement field u_i, which represents the displacement of the material points in the medium from their steady-state positions. The velocity field in the solid layer is $v_i = \partial_t u_i$. In an incompressible linear viscoelastic solid, the displacement field satisfies the continuity equation

$$\partial_i u_i = 0. \tag{6}$$

The momentum conservation equation is given by

$$\mathrm{Re}\ \partial_t^2 u_i = \partial_j \Pi_{ij}, \tag{7}$$

where $\Pi_{ij} = -p_g \delta_{ij} + \sigma_{ij}$ is the total stress tensor which is given by a sum of the isotropic pressure p_g and deviatoric stress σ_{ij}. Without loss of generality, it is assumed here that the density of the solid is equal to the density of the two fluids. The deviatoric stress tensor σ_{ij} is given by a sum of elastic and viscous stresses in the solid layer:

$$\sigma_{ij} = \left(\frac{1}{\Gamma} + \eta_r \partial_t\right)(\partial_i u_j + \partial_j u_i), \tag{8}$$

where $\Gamma = V\mu_b/(GR)$ is the nondimensional parameter characterizing the elasticity of the solid layer and $\eta_r = \eta_w/\mu_b$ is the ratio of solid to fluid B viscosities. More precisely, $1/\Gamma$ is the estimated ratio of elastic stresses in the solid layer to viscous stresses in the fluid B. The solid layer is assumed to be fixed to a rigid surface at $z=-H$, and the boundary condition for the displacement field there is $u_i=0$. A recent study by Gkanis and Kumar[17] on the stability of the single-layer plane Couette flow of a Newtonian fluid past a deformable solid has examined the role of nonlinear rheological properties in the solid by modeling the deformable solid using the neo-Hookean model. This study shows that for nonzero interfacial tension between the fluid and the solid medium, and sufficiently large values of solid layer thickness ($H \geqslant 2$), the results from both linear and nonlinear solid models agree quite well, while for smaller values of solid thickness, the linear model significantly overpredicts the critical velocity required for destabilizing the flow. It is demonstrated later in this paper that the linear viscoelastic model is expected to yield accurate results for the present study, and hence we employ this simple model to describe the deformation in the solid layer.

The conditions at the interface $z=g(x)$ (see Fig. 1) between the two Newtonian fluids are the continuity of velocities and stresses, and the kinematic condition for the evolution of the interface position $g(x)$. We include the effect of nonzero interfacial tension γ between the two fluids at this interface. The conditions at the interface $z=h(x)$ between fluid B and the solid layer are the continuity of velocities and stresses. We neglect the effect of interfacial tension between fluid B and the solid layer, as this was found in the earlier study of Kumaran *et al.*[3] to have a purely stabilizing effect on the interfacial mode of the interface $z=h(x)$ between the fluid and the solid layer.

B. Base state

The steady velocity profiles in the two fluids are simply the Couette flow velocity profiles, with different gradients due to the difference in viscosities of the two fluids:

$$\overline{v_x^a} = \frac{z + \beta(\mu_r - 1)}{1 + \beta(\mu_r - 1)}, \quad \overline{v_x^b} = \frac{\mu_r z}{1 + \beta(\mu_r - 1)}, \tag{9}$$

where the base flow quantities are denoted with an overbar. The solid layer is at rest in this steady base state, but there is a nonzero unidirectional displacement $\overline{u_x}$ due to the fluid shear stresses at the interface:

$$\overline{u_x} = \frac{\mu_r \Gamma (z + H)}{1 + \beta(\mu_r - 1)}. \tag{10}$$

C. Linear stability analysis

Small perturbations (denoted by primed quantities) are introduced to the fluid velocity about the base state, $v_i^\alpha = \overline{v_i^\alpha} + v_i^{\alpha\prime}$, and other dynamical quantities in the two fluids and the solid layer are similarly perturbed. A temporal stability analysis is used to determine the fate of small perturbations to the above base state. All the perturbation quantities are expanded in the form of Fourier modes in the x direction, and with an exponential dependence in time:

$$v_i^{\alpha\prime} = \tilde{v}_i^\alpha(z)\exp[ik(x - ct)], \quad u_i' = \tilde{u}_i(z)\exp[ik(x - ct)],$$

$$\alpha = a, b, \tag{11}$$

where k is the wavenumber, c is the wavespeed which is a complex number, and $\tilde{v}_i^\alpha(z)$ and $\tilde{u}_i(z)$ are eigenfunctions which are determined below from the linearized governing equations and boundary conditions. For simplicity, only two-dimensional perturbations are considered. The complex wavespeed is $c=c_r+ic_i$, and when $c_i>0$, the base state is temporally unstable.

Upon substituting the above form for the perturbations in the governing equations for the two fluids, Eqs. (1) and (2), we obtain the following linearized stability equations for the two fluids, where $\alpha=a,b$ and $d_z=d/dz$:

$$d_z\tilde{v}_z^\alpha + ik\tilde{v}_x^\alpha = 0, \tag{12}$$

$$ik\,\mathrm{Re}(\overline{v_x^\alpha} - c)\tilde{v}_x^\alpha + \mathrm{Re}\,(d_z\overline{v_x^\alpha})\tilde{v}_z^\alpha = -ikp^\alpha + \mu_r^\alpha(d_z^2 - k^2)\tilde{v}_x^\alpha, \tag{13}$$

$$ik\,\mathrm{Re}(\overline{v_x^\alpha} - c)\tilde{v}_z^\alpha = -d_z p^\alpha + \mu_r^\alpha(d_z^2 - k^2)\tilde{v}_z^\alpha. \tag{14}$$

The above equations can be combined to give a single fourth-order, Orr–Sommerfeld-like equation for $\tilde{v}_z^\alpha$:

$$ik\,\mathrm{Re}(\overline{v_x^\alpha} - c)(d_z^2 - k^2)\tilde{v}_z^\alpha = \mu_r^\alpha(d_z^2 - k^2)^2\tilde{v}_z^\alpha. \tag{15}$$

The governing equations for the displacement field in the solid layer can be expressed in terms of $\tilde{u}_i(z)$ in a similar manner to give

$$d_z\tilde{u}_z + ik\tilde{u}_x = 0, \tag{16}$$

$$-\mathrm{Re}\,k^2c^2\tilde{u}_x = -ik\tilde{p}_g + \left(\frac{1}{\Gamma} - ikc\eta_r\right)(d_z^2 - k^2)\tilde{u}_x, \tag{17}$$

$$-\mathrm{Re}\,k^2c^2\tilde{u}_z = -d_z\tilde{p}_g + \left(\frac{1}{\Gamma} - ikc\eta_r\right)(d_z^2 - k^2)\tilde{u}_z. \tag{18}$$

These equations can be reduced to a single fourth-order differential equation for $\tilde{u}_z$:

$$(1 - ikc\eta_r\Gamma)(d_z^2 - k^2)^2\tilde{u}_z + \mathrm{Re}\,k^2c^2\Gamma(d_z^2 - k^2)\tilde{u}_z = 0. \tag{19}$$

The linearized boundary conditions at the unperturbed interface position $z=0$ between fluid B and the solid layer are obtained by Taylor expanding about the flat interface position in the base state.[3] These become

$$\tilde{v}_z^b = (-ikc)\tilde{u}_z, \tag{20}$$

$$\tilde{v}_x^b + [d_z\overline{v_x^b}]_{z=0}\tilde{u}_z = (-ikc)\tilde{u}_x, \tag{21}$$

$$-\tilde{p}^b + \tilde{\tau}_{zz}^b = -\tilde{p}_g + \left(\frac{1}{\Gamma} - ikc\eta_r\right)2d_z\tilde{u}_z, \tag{22}$$

$$(d_z\tilde{v}_x^b + ik\tilde{v}_z^b) = \left(\frac{1}{\Gamma} - ikc\,\eta_r\right)(d_z\tilde{u}_x + ik\tilde{u}_z). \tag{23}$$

Here, the second term in the left side of Eq. (21) represents the nontrivial contribution that arises as a result of the Taylor expansion of the mean flow quantities about the unperturbed fluid–solid interface. This additional term is responsible for the instability of the interface between the fluid and the deformable solid layer.[3]

Similarly, the linearized boundary conditions at the unperturbed interface position at $z=\beta$ between the two fluids A and B are given by (see, for example, Ref. 11)

$$\tilde{v}_z^a = \tilde{v}_z^b, \tag{24}$$

$$\tilde{v}_x^a + [d_z\overline{v}_x^a]_{z=\beta}\tilde{g} = \tilde{v}_x^b + [d_z\overline{v}_x^b]_{z=\beta}\tilde{g}, \tag{25}$$

$$\mu_r[d_z\tilde{v}_x^a + ik\tilde{v}_z^a] = [d_z\tilde{v}_x^b + ik\tilde{v}_z^b], \tag{26}$$

$$-\tilde{p}^a + 2\mu_r d_z\tilde{v}_z^a - \Sigma k^2\tilde{g} = -\tilde{p}^b + 2d_z\tilde{v}_z^b, \tag{27}$$

where $\tilde{g}$ is the Fourier expansion coefficient for the interface position $g=\tilde{g}\exp[ik(x-ct)]$, and $\Sigma=\gamma/(\mu_b V)$ is the nondimensional interfacial tension between fluids A and B. Note that in the tangential velocity condition [Eq. (25)], there are additional terms that arise due to Taylor expansion because of the discontinuity in the velocity gradient at $z=\beta$ in the base state. The linearized kinematic condition at $z=\beta$ between the two fluids is given by

$$ik[\overline{v}_x^a(z=\beta) - c]\tilde{g} = \tilde{v}_z^a. \tag{28}$$

The boundary conditions at $z=1$ are simply

$$\tilde{v}_z^a = 0,\ \ \tilde{v}_x^a = 0, \tag{29}$$

while the boundary conditions at $z=-H$ are

$$\tilde{u}_z = 0,\ \ \tilde{u}_x = 0. \tag{30}$$

Differential equations (15) and (19) along with boundary conditions (20)–(30) completely specify the stability problem for the three-layer configuration of interest in this study. The complex wavespeed c is a function of Re, Γ, k, H, β, Σ, η_r, and μ_r. For arbitrary Re and k, there are no closed form solutions to the fourth-order differential equation (15), and so a numerical method must be used to solve the stability problem in general. However, when we consider very long waves, i.e., $k\ll 1$, an asymptotic analysis in the small parameter k is possible, similar to the analysis of Yih,[10] which yields an analytical expression for the wavespeed as an asymptotic series in k. In the following section, we briefly outline the low wavenumber asymptotic analysis and the results obtained from that analysis. These low k results are then used as starting guesses for a complete numerical treatment of the stability problem in Sec. IV.

III. LOW WAVENUMBER ANALYSIS

In this section, the effect of a third solid layer on the stability of the two-layer plane Couette flow is studied in the limit $k\ll 1$. The low wavenumber (or long wavelength) asymptotic analysis which includes the effect of the third solid layer is similar, but not identical, to the analysis of Yih.[10] For $k\ll 1$, the complex wavespeed c is expanded in an asymptotic series in k:

$$c = c^{(0)} + kc^{(1)} + \cdots. \tag{31}$$

If we set $\tilde{v}_z^\alpha \sim O(1)$, then the continuity equation (12) implies $\tilde{v}_x^\alpha \sim k^{-1}\tilde{v}_z^\alpha$, and the x momentum equation (13) implies $\tilde{p}^\alpha \sim k^{-2}\tilde{v}_z^\alpha$. Therefore, the velocities and the pressure in the two fluids are expanded as

$$\tilde{v}_z^\alpha = \tilde{v}_z^{\alpha(0)} + k\tilde{v}_z^{\alpha(1)} + \cdots, \tag{32}$$

$$\tilde{v}_x^\alpha = \frac{1}{k}\tilde{v}_x^{\alpha(0)} + \tilde{v}_x^{\alpha(1)} + \cdots, \tag{33}$$

$$\tilde{p}^\alpha = \frac{1}{k^2}\tilde{p}^{\alpha(0)} + \frac{1}{k}\tilde{p}^{\alpha(1)} + \cdots. \tag{34}$$

For the present system, our subsequent analysis indicates that $c^{(1)}$ determines the stability of the problem, and so only the leading order and first correction to various dynamical quantities are required in the following analysis. The displacement field and the pressure in the solid layer are expanded in a similar manner:

$$\tilde{u}_z = \tilde{u}_z^{(0)} + k\tilde{u}_z^{(1)} + \cdots, \tag{35}$$

$$\tilde{u}_x = \frac{1}{k}\tilde{u}_x^{(0)} + \tilde{u}_x^{(1)} + \cdots, \tag{36}$$

$$\tilde{p}_g = \frac{1}{k^2}\tilde{p}_g^{(0)} + \frac{1}{k}\tilde{p}_g^{(1)} + \cdots. \tag{37}$$

Upon substituting the asymptotic expansions (31)–(37) in the governing equations (15) and (19), we obtain the following differential equations that determine the leading order and first correction to the fluid velocity fields ($\alpha=a,b$):

$$\mu_r^\alpha d_z^4\tilde{v}_z^{\alpha(0)} = 0, \tag{38}$$

$$\mu_r^\alpha d_z^4\tilde{v}_z^{\alpha(1)} = i\,\mathrm{Re}(\overline{v}_x^\alpha - c^{(0)})d_z^2\tilde{v}_z^{\alpha(0)}. \tag{39}$$

The leading order and first correction to the pressure in the two fluids are given by

$$\tilde{p}^{\alpha(0)} = -i\mu_r^\alpha d_z^2\tilde{v}_x^{\alpha(0)}, \tag{40}$$

$$\tilde{p}^{\alpha(1)} = -i[\mu_r^\alpha d_z^2\tilde{v}_x^{\alpha(1)} - i\,\mathrm{Re}(\overline{v}_x^\alpha - c^{(0)})\tilde{v}_x^{\alpha(0)} - \mathrm{Re}(d_z\overline{v}_x^\alpha)\tilde{v}_z^{\alpha(0)}]. \tag{41}$$

The original differential equation (15) describing the linear stability in the two fluids is a fourth-order differential equation, and so has four linearly independent solutions. In what follows, we obtain the leading order and $O(k)$ contribution to the four linearly independent solutions by solving the differential equations at each order, and substitute the asymptotic expansions in the boundary and interface conditions, which will then determine the wavespeed. The leading order differential equation for $\tilde{v}_z^{\alpha(0)}$ [Eq. (38)] is integrated to obtain

$$\tilde{v}_z^{a(0)} = A_1 z^3 + A_2 z^2 + A_3 z + A_4, \tag{42}$$

$$\tilde{v}_z^{b(0)} = B_1 z^3 + B_2 z^2 + B_3 z + B_4, \tag{43}$$

where $\{A_1,\ldots,A_4\}$ and $\{B_1,\ldots,B_4\}$ are constants of integration which will be determined after satisfying the boundary and interface conditions. The solution to the differential equation governing the first correction to the fluid velocities, Eq. (39), is also analytically obtained:

$$\tilde{v}_z^{a(1)} = \frac{-A_1 i\,\mathrm{Re}[3c^{(0)} + 3\beta(-1+c^{(0)})(-1+\mu_r) - z]z^5}{60[1+\beta(-1+\mu_r)]\mu_r} + \frac{-A_2 i\,\mathrm{Re}[5c^{(0)} + 5\beta(-1+c^{(0)})(-1+\mu_r) - z]z^4}{60[1+\beta(-1+\mu_r)]\mu_r}, \tag{44}$$

$$\tilde{v}_z^{b(1)} = \frac{B_1 i\,\mathrm{Re}\, z^5\{-3c^{(0)}[1+\beta(-1+\mu_r)] + \mu_r z\}}{60[1+\beta(-1+\mu_r)]} + \frac{B_2 i\,\mathrm{Re}\, z^4\{-5c^{(0)}[1+\beta(-1+\mu_r)] + \mu_r z\}}{60[1+\beta(-1+\mu_r)]}. \tag{45}$$

Note that the inhomogeneous term in the right side of Eq. (39) is nonzero only for the leading order solutions A_1z^3 and A_2z^2, and so the constants A_3 and A_4 do not appear in the solution for the first correction $\tilde{v}_z^{a(1)}$. A similar argument applies for the solution $\tilde{v}_z^{b(1)}$.

Subsequent analysis shows that the leading order displacement and pressure fields in the solid layer are sufficient for the present problem. Upon substituting the expansion for $\tilde{u}_z$ [Eq. (35)] in the fourth-order differential equation [Eq. (19)] governing the solid deformation, we obtain to leading order in k

$$d_z^4\tilde{u}_z^{(0)} = 0, \quad \tilde{p}_g^{(0)} = -\frac{i}{\Gamma}d_z^2\tilde{u}_x^{(0)}. \tag{46}$$

In the present analysis, the solid elasticity parameter Γ is assumed to be an $O(1)$ quantity as $k\to 0$, i.e., this parameter does not scale with k for $k\ll 1$. The solution of the above equation, after satisfying the two boundary conditions at $z=-H$ [Eq. (30)], is given by

$$\tilde{u}_z^{(0)} = D_2(H^2 + 2Hz + z^2) + D_1(-2H^3 - 3H^2z + z^3). \tag{47}$$

The leading order and first correction solutions to the velocity and pressure fields in the two fluid layers, and the solution to the leading order displacement and pressure fields in the solid layer are inserted in the asymptotic expansions [Eqs. (31)–(37)], which are then substituted in the boundary and interface conditions [Eqs. (20)–(29)]. These can be expressed in the following matrix form:

$$\mathbf{M}\cdot\mathbf{C}^T = 0, \tag{48}$$

where $\mathbf{C}=\{A_1,A_2,A_3,A_4,B_1,B_2,B_3,B_4,D_1,D_2\}$ is the vector of coefficients and $\mathbf{M}$ is a 10×10 matrix whose rows represent the different interface and boundary conditions. The characteristic equation is obtained by setting the determinant of the matrix $\mathbf{M}$ to zero. In the low wavenumber asymptotic analysis, the determinant of this matrix is expanded in a series in k, as follows:

$$f_0(c^{(0)}) + kf_1(c^{(0)},c^{(1)}) + \cdots = 0, \tag{49}$$

where f_0 is the leading order term in the determinant and f_1 is the first correction. The leading order, first correction, and higher order terms must be separately zero for the determinant to be zero, i.e.,

$$f_0(c^{(0)}) = 0, \quad f_1(c^{(0)},c^{(1)}) = 0, \ldots. \tag{50}$$

These algebraic equations can then be sequentially solved to obtain expressions for $c^{(0)}$ and $c^{(1)}$. The above procedure was implemented using the symbolic package MATHEMATICA, and we first verified that the results from our analysis for the case of two-layer plane Couette flow without the solid layer agree exactly with the results of Yih.[10] We compared our expression for $c^{(0)}$ with Yih's expression and our results for $c^{(1)}$ with Fig. 2(a) of Yih, and found exact agreement.

For the three-layer configuration of interest in this study, our asymptotic analysis shows that at leading order, $c^{(0)}$ is purely real, and is identical to Yih's[10] result for leading order wavespeed in the two-layer plane Couette flow system. In other words, the solid layer does not appear at the leading order problem in the present three-layer configuration. Thus, in order to determine the stability of the system, one must calculate the first correction $c^{(1)}$. Our asymptotic analysis shows that in the $k\to 0$ limit, the parameters Σ (interfacial tension) and η_r (solid to fluid viscosity ratio) do not appear in $c^{(0)}$ and $c^{(1)}$. The analytical expression for $c^{(1)}$ is very complicated when the remaining parameters Re, Γ, μ_r, H, and β are left unspecified. However, when only β and μ_r are specified, it is possible to obtain analytical expressions for $c^{(1)}$ with the other parameters left unspecified. For example, when $\beta=0.4$, $\mu_r=0.5$, the results for $c^{(0)}$ and $c^{(1)}$ from our analysis are

$$c^{(0)} = 0.314\,47, \tag{51}$$

$$c^{(1)} = i[\mathrm{Re}(1.2\times 10^{-4}) - 0.034\,27\Gamma H(H^2 + 2.2421H + 1.498\,36)]. \tag{52}$$

The result for $c^{(0)}$ is identical to that of Yih[10] for the case of two-layer Couette flow without the solid layer, and is purely real. The first correction $c^{(1)}$, however, is purely imaginary, and has two contributions: the term proportional to Re is destabilizing and is identical to the result of Yih. However, there is another term proportional to Γ and H which appears at this order due to the presence of the solid layer. The solid elasticity parameter $\Gamma = V\mu_b/(GR)$ tends to zero in the limit of a rigid solid layer (i.e., the shear modulus G of the solid layer becomes large compared to the viscous shear stresses in the fluid B, $\mu_b V/R$). However, as the shear modulus G decreases, Γ increases, thus making the solid layer more deformable. The parameter H is the nondimensional thickness of the solid layer. For $\beta=0.4$, $\mu_r=0.5$, our asymptotic analysis thus shows that when Γ and H are nonzero, the solid layer has a stabilizing effect on the longwave instability due to viscosity stratification. The expression for $c^{(1)}$ shows, as would be expected, that the stabilizing nature of the solid

layer vanishes when $\Gamma=0$ (the case of a rigid solid layer) or $H=0$ (the case of no solid layer). From the above expression, the value of Γ required for neutrally stable modes is obtained by setting $c^{(1)}$ to zero:

$$\Gamma_{c0}=\frac{3.502\times10^{-3}\,\mathrm{Re}}{H(H^2+2.2421H+1.498\,36)}. \tag{53}$$

When $\Gamma>\Gamma_{c0}$ (the subscript "0" refers to the low wavenumber asymptotic result), the longwave instability due to viscosity stratification at the two-fluid interface is stabilized. It is useful to define a new nondimensional parameter $\Lambda\equiv\mathrm{Re}/\Gamma=\rho GR^2/\mu_b^2$ which is a flow independent nondimensional elasticity of the solid layer. Using this parameter Λ, the two-fluid interfacial instability will be stabilized for $\beta=0.4$ and $\mu_r=0.5$ when

$$\Lambda<285.5H(H^2+2.2421H+1.498\,36). \tag{54}$$

For $H=0.5$, $\Lambda<410$ for stability, while for $H=4$, $\Lambda<3\times10^4$ for stability of the two-fluid interface. It is useful at this point to estimate the parameter Λ in a typical application: when $G=10^5$ Pa, $\rho=10^3$ kg m^{-3}, $R=10^{-2}$ m and $\mu_b=10$ kg m^{-1} s^{-1}, $\Lambda\sim100$, which is lower than 410. Thus, it should be possible to experimentally realize the predicted stabilization for two-layer flow of more viscous fluids flowing past soft elastomeric solids. However, in experimental studies, it may be important to ascertain whether such soft solids undergo fracture due to the fluid stresses. The interfacial mode between fluid *B* and the solid layer (mode 2) is a finite wavelength instability which remains stable as $k\to0$ when $\Gamma\sim O(1)$. Therefore, for $k\ll1$, both the modes remain stable when $\Gamma>\Gamma_{c0}$.

We now consider the configuration in which we increase β from 0.4 to 0.7, with $\mu_r=0.5$. In this case, the thickness of the more viscous fluid is larger compared to that of the less viscous fluid. The long wave analysis of Yih predicts that such a configuration is *stable* for two-layer plane Couette flow. Our asymptotic result, with the inclusion of the third solid layer, for $\mu_r=0.5$ and $\beta=0.7$ is given by

$$c^{(0)}=0.614\,861, \tag{55}$$

$$c^{(1)}=i[-\mathrm{Re}(1.52\times10^{-4})+\Gamma H0.025\,69(H-0.2862)(H+0.8009)]. \tag{56}$$

For this case again, $c^{(1)}$ has two contributions, one proportional to Re and the other proportional to ΓH. The term proportional to Re is stabilizing, and is identical to the result of Yih for two-layer plane Couette flow. The term proportional to ΓH represents the effect of the solid layer on the two-fluid mode 1, and this term is stabilizing if $H<0.2862$, and is destabilizing for $H>0.2862$. Thus, this example illustrates that the solid layer could have a destabilizing effect on the two-fluid interfacial mode when the solid layer is sufficiently thick.

In general, therefore, the results of the low wavenumber analysis can be expressed as follows:

TABLE I. Qualitative summary of results from low wavenumber analysis for $\mu_r=0.25$.

β	$F(H)$	C_1
0.1	stable for all H	1.329×10^{-4}
0.2	stable for all H	4.59×10^{-4}
0.3	stable for all H	6.706×10^{-4}
0.4	stable for all H	4.986×10^{-4}
0.5	stable for all H	7.565×10^{-5}
0.6	stable for all H	-2.827×10^{-4}
0.7	stable for $H<2.598$ unstable for $H>2.598$	-4.415×10^{-4}
0.9	unstable for all H	-2.6049×10^{-4}

$$c=c^{(0)}+ki[\Gamma HF(H)+\mathrm{Re}\,C_1], \tag{57}$$

where $c^{(0)}$ is purely real, $F(H)$ is a real-valued function of H (which can be positive or negative depending on H) that represents the effect of the solid layer, and C_1 is a real constant that represents the contribution due to the viscosity stratification between the two fluids, and is identical to Yih's result. A few representative results for $F(H)$ and C_1 are qualitatively summarized for different values of μ_r and β in Tables I–IV. From these results (and from the results for other values of β and μ_r which are not presented here), the general trend appears to be that when the two fluid layers are arranged so that they undergo the long-wave two-layer viscosity stratification instability, the solid layer usually has a stabilizing effect in the long-wave limit. On the other hand, when the two fluid layers are arranged so that the interface is stable in the long-wave limit, then the solid layer usually has a destabilizing effect, but for certain values of H, it could further stabilize the two-fluid interfacial perturbations. The low k asymptotic results also reveal interestingly that the stabilizing or destabilizing effect of the solid layer depends crucially on the placement of the two fluid layers with respect to the solid layer. For example, the result for $\mu_r=0.5$ and $\beta=0.6$ (see Table III; the case where the more viscous

TABLE II. Qualitative summary of results from low wavenumber analysis for $\mu_r=4$.

β	$F(H)$	C_1
0.1	unstable for all H	-6.512×10^{-5}
0.3	unstable for all H	-1.104×10^{-4}
0.4	unstable for $H<1.22$ stable for $H>1.22$	-7.069×10^{-5}
0.5	unstable for $H<0.1$ stable for $H>0.1$	1.189×10^{-5}
0.6	stable for all H	1.246×10^{-4}
0.7	stable for all H	1.676×10^{-4}
0.8	stable for all H	1.147×10^{-4}
0.9	stable for all H	3.32×10^{-5}

TABLE III. Qualitative summary of results from low wavenumber analysis for $\mu_r=0.5$.

β	$F(H)$	C_1
0.1	stable for all H	6.811×10^{-5}
0.2	stable for all H	1.781×10^{-4}
0.3	stable for all H	2.006×10^{-4}
0.4	stable for all H	1.2×10^{-4}
0.5	stable for all H	2.86×10^{-6}
0.6	stable for $H<7.92$ unstable for $H>7.92$	-9.6×10^{-5}
0.7	stable for $H<0.286$ unstable for $H>0.286$	-1.527×10^{-4}
0.8	unstable for all H	-1.553×10^{-4}
0.9	unstable for all H	-9.504×10^{-5}

fluid of larger thickness is adjacent to the solid layer) shows that the solid layer has a stabilizing effect for $H<7.92$ and becomes destabilizing for $H>7.92$. If the two fluid layers are interchanged, i.e., if the less viscous fluid of smaller thickness is adjacent to the solid layer ($\mu_r=2, \beta=0.4$), then the effect of the solid layer is very different (see Table IV), and is destabilizing for all values of H.

It is useful at this point to remark on the possible physical mechanism of the stabilization/destabilization of the two-fluid mode by the deformable solid. The low-wavenumber asymptotic result for the wavespeed c [Eq. (57)] provides the clue to understand the effect of the solid layer on the two-fluid mode. To this end, it is useful to consider the two different contributions to the first correction to c separately. First, consider the case of two-layer flow in a rigid channel ($\Gamma=0$ or $H=0$), and in this case, C_1 determines whether the two-fluid mode is stable or unstable. The term C_1 is caused by the first correction [at $O(k)$] to the velocity field in both the fluids, which is also proportional to Re. It has been demonstrated by Charru and Hinch[16] using a very detailed analysis that this first correction velocity field in the two fluids can

TABLE IV. Qualitative summary of results from low wavenumber analysis for $\mu_r=2$.

β	$F(H)$	C_1
0.1	unstable for all H	-4.75×10^{-4}
0.2	unstable for all H	-7.76×10^{-5}
0.3	unstable for all H	-7.63×10^{-5}
0.4	unstable for all H	-4.80×10^{-5}
0.5	unstable for $H<0.865$ stable for $H>0.865$	1.43×10^{-6}
0.6	stable for all H	6.002×10^{-4}
0.7	stable for all H	1.003×10^{-4}
0.8	stable for all H	8.906×10^{-5}
0.9	stable for all H	3.406×10^{-5}

set up a flow in such a manner that the perturbations of the two-fluid interface can be amplified or suppressed under appropriate conditions. At $\mathrm{Re}=0$, the first correction to the velocity field vanishes, and the two-layer flow is neutrally stable. Next, consider the case of two-layer flow past a deformable solid layer ($\Gamma\neq0, H\neq0$) at $\mathrm{Re}=0$. In the absence of fluid inertia, the first correction velocity field proportional to Re clearly vanishes. However, the presence of interfacial oscillations at the fluid-deformable solid interface sets up a velocity field at $O(k)$ in both the fluids, and this perturbation velocity field due to wall oscillations can, under appropriate conditions (which are precisely determined by the low-wavenumber analysis), act in a way so as to amplify or suppress the two-fluid interfacial fluctuations. When both $\mathrm{Re}\neq0$ and $\Gamma\neq0$ (i.e., finite fluid inertia and nonzero solid layer deformability), both the above mechanisms are present, and they can be stabilizing or destabilizing. The result for $c^{(1)}$ [Eq. (57)] is a mathematical expression of these two different effects.

The above asymptotic results, however, are applicable only in the low k limit. In order to determine whether the predicted stabilization extends to perturbations with finite and high k, it is necessary to solve the governing stability equations and boundary conditions numerically. In addition, at finite k, the interfacial mode at the fluid B–solid interface can become unstable when Γ is increased beyond a critical value. In the following section, we use the numerical solution to determine regions in the Γ-k plane where both the interfacial modes are stable.

IV. RESULTS FROM NUMERICAL SOLUTION

A. Numerical method

We first briefly outline the method used to solve the three layer configuration of interest here. There are three fourth-order ordinary differential equations (ODEs) in the two fluid layers and the solid layer. We use a fourth-order Runge–Kutta integrator with adaptive step size control to obtain numerical representations of the linearly independent solutions to the fourth-order ODEs. We recast the fourth order ODE in each layer as a system of first-order differential equations (see, for example, Drazin and Reid,[22] Chap. 4) for the variables $[\tilde{v}_z, d_z\tilde{v}_z, d_z^2\tilde{v}_z, d_z^3\tilde{v}_z]$. For fluid A, this system of first-order equations can be integrated from $z=1$ to $z=\beta$, provided the values of $\tilde{v}_z$ and its first three derivatives are known at $z=1$. For layer A, the fluid velocity satisfies the boundary conditions $\tilde{v}_z=0$ and $\overline{v_x}=i/kd_z\tilde{v}_z=0$ at $z=1$. We use two different sets of higher derivatives $d_z^2\tilde{v}_z$ and $d_z^3\tilde{v}_z$ at $z=1$ that are consistent with the boundary conditions at $z=1$, which will yield the two linearly independent solutions to the fluid velocity field in fluid A:

$$\tilde{v}_z=0,\ \ d_z\tilde{v}_z=0,\ \ d_z^2\tilde{v}_z=1,\ \ d_z^3\tilde{v}_z=0, \tag{58}$$

$$\tilde{v}_z=0,\ \ d_z\tilde{v}_z=0,\ \ d_z^2\tilde{v}_z=0,\ \ d_z^3\tilde{v}_z=1. \tag{59}$$

Using these conditions at $z=1$, we use the Runge–Kutta method to integrate the ODE in fluid A up to $z=\beta$. The velocity field $\tilde{v}_z$ in fluid A is then obtained as a linear combination of these two solutions (denoted by $\tilde{v}_z^{a(1)}$ and $\tilde{v}_z^{a(2)}$),

and this velocity field is consistent with the boundary conditions at $z=1$:

$$\tilde{v}_z^a = A_1 \tilde{v}_z^{a(1)} + A_2 \tilde{v}_z^{a(2)}. \tag{60}$$

Here, A_1 and A_2 are constants which have to be determined by the interface conditions at $z=\beta$. For fluid layer B, which is bounded by fluid A and solid on both sides, we obtain *four* linearly independent solutions by using four different sets of "initial conditions" at $z=\beta$:

$$\tilde{v}_z = 1,\ d_z\tilde{v}_z = 0,\ d_z^2\tilde{v}_z = 0,\ d_z^3\tilde{v}_z = 0, \tag{61}$$

$$\tilde{v}_z = 0,\ d_z\tilde{v}_z = 1,\ d_z^2\tilde{v}_z = 0,\ d_z^3\tilde{v}_z = 0, \tag{62}$$

$$\tilde{v}_z = 0,\ d_z\tilde{v}_z = 0,\ d_z^2\tilde{v}_z = 1,\ d_z^3\tilde{v}_z = 0, \tag{63}$$

$$\tilde{v}_z = 0,\ d_z\tilde{v}_z = 0,\ d_z^2\tilde{v}_z = 0,\ d_z^3\tilde{v}_z = 1. \tag{64}$$

Using these four conditions at $z=\beta$, we obtain four linearly independent solutions by numerical integration up to $z=0$. The velocity field in fluid B is obtained as a linear combination of the four solutions.

The solid displacement field satisfies $\tilde{u}_z=0$ and $\tilde{u}_x = i/kd_z\tilde{u}_z=0$ at $z=-H$. Therefore, we choose the following initial conditions at $z=-H$ consistent with the boundary conditions for the displacement field

$$\tilde{u}_z = 0,\ d_z\tilde{u}_z = 0,\ d_z^2\tilde{u}_z = 1,\ d_z^3\tilde{u}_z = 0, \tag{65}$$

$$\tilde{u}_z = 0,\ d_z\tilde{u}_z = 0,\ d_z^2\tilde{u}_z = 0,\ d_z^3\tilde{u}_z = 1. \tag{66}$$

Using the above conditions, we integrate the ODE in the solid layer up to $z=0$, and the displacement field in the solid is obtained as a linear combination of the two solutions. Thus, there are eight coefficients (two in layer A, four in layer B, and two in the solid layer) multiplying the linearly independent solutions in the three layers. The numerical solutions obtained in this manner are substituted in the eight interface conditions at $z=0$ [Eqs. (20)–(23)] and $z=\beta$ [Eqs. (24)–(27)] and an 8×8 characteristic matrix is obtained, whose determinant is set to zero to obtain the characteristic equation. A Newton–Raphson iteration technique is used to solve the characteristic equation and obtain the complex wavespeed, for specified values of k, β, H, η_r, μ_r, Σ, Γ, and Re. It is important to note that at nonzero Re, the characteristic equation is not a simple polynomial in c, because the wavespeed occurs in the Orr–Sommerfeld equations of the fluids as well. Also, there could be many stable solutions to c at low (but finite) Re to the fluid-solid problem, which are not of interest in the present study. Here, we are interested in the behavior of the two "interfacial modes," respectively, at the two interfaces, and the effect of solid layer deformability on these modes.

We use the low k asymptotic results for mode 1 as starting guesses for the numerical procedure, and continue the low k results numerically to finite and high values of k. For mode 2 (the fluid B–solid interfacial mode), we use results from a zero Re analysis for the present three-layer configuration (which gives analytical solutions for the wavespeed) as starting guesses and continue the results to finite Re. We have validated the above numerical procedure by comparing our results with those of Shankar and Kumaran[9] who studied numerically the stability of single layer Newtonian Couette flow past a deformable solid at finite Re. The results of Shankar and Kumaran are recovered when $\mu_r=1$ and $\Sigma=0$ in the present formulation. We also compared the results from numerical code obtained for low k with the asymptotic (analytical) results of the preceding section, and found excellent agreement.

B. Results

It is first instructive to briefly recapitulate the results of Yih[10] for the case of two-layer Couette flow in rigid-walled channels. Yih's long wave analysis showed that this configuration is unstable if the thickness of the more viscous fluid is smaller than that of the less viscous fluid. For the opposite case, viz., when the thickness of the less viscous fluid is smaller than that of the more viscous fluid, the two-layer flow is stable (this phenomenon is referred to as the "thin layer effect;" see, for example, Ref. 11). Using the numerical procedure described above, it is possible to recover the case of two-layer flow in rigid channels by setting the parameter $\Gamma=0$, and to obtain the variation for c_r and c_i vs k for all k. The results of the low wavenumber asymptotic analysis are used as starting guesses for this numerical solution. Figures 2(a) and 2(b), respectively, show the variation of c_r and c_i with k for two thickness ratios, one which is unstable in the low wavenumber limit, and the other configuration is stable in the low wavenumber limit. Figure 2(b) shows that for $\beta=0.4$, c_i reaches a maximum for $k\sim O(1)$, and it remains unstable even for large k since the interfacial tension $\Sigma=0$ in this case. For $\beta=0.8$, the more viscous fluid is of larger thickness, and so the configuration is stable for low k and finite k. However, at large k, this configuration also becomes unstable, and c_i for $\beta=0.8$ tends to approach the c_i predicted for $\beta=0.4$. This result is consistent with the short wave asymptotic analysis of Hooper and Boyd,[15] who showed that the interface between the shear flow of two fluids with viscosity stratification is always unstable to short waves, regardless of the thickness of the two fluids. This is because, for very short waves, the interfacial perturbations are localized near the two-fluid interface, and so the thickness ratio of the two fluids should not have an effect on c_i vs k. However, the presence of nonzero interfacial tension stabilizes short wavelength perturbations, and this is shown in Fig. 3. In this case, only the configuration that is unstable ($\beta=0.4$) for low k exhibits the interfacial instability for low and finite k, while for $\beta=0.8$, the short wave instability is stabilized by nonzero Σ. For $\beta=0.4$ and $\Sigma=0$, we have further verified that for low k, $c_i\propto k$, in agreement with Yih's low k asymptotic analysis, while for high k, $c_i\propto k^{-3}$ (for $\Sigma=0$), in agreement with Hooper and Boyd's high k asymptotic analysis. We refer to this interfacial mode between the two fluids as "mode 1" in the following discussion.

Before turning to the effect of the solid layer on the two-fluid interfacial instability, it is useful to briefly recall the results of Kumaran *et al.*[3] who studied the stability of the interface between a single-layer Newtonian fluid past a de-

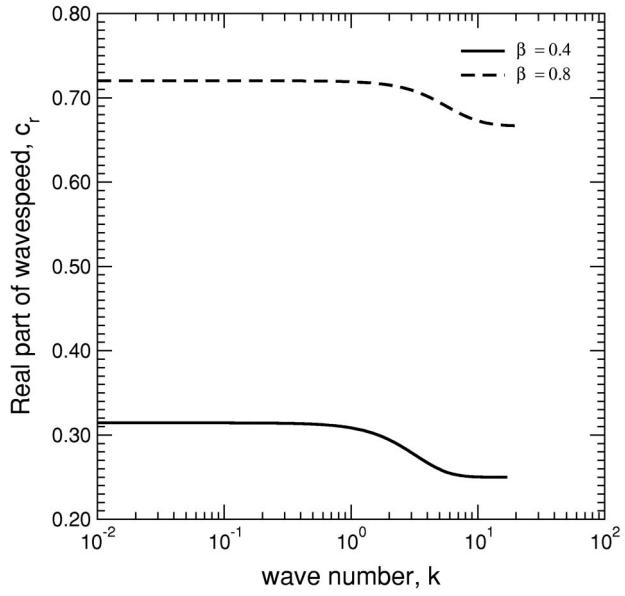

(a) c_r vs. k

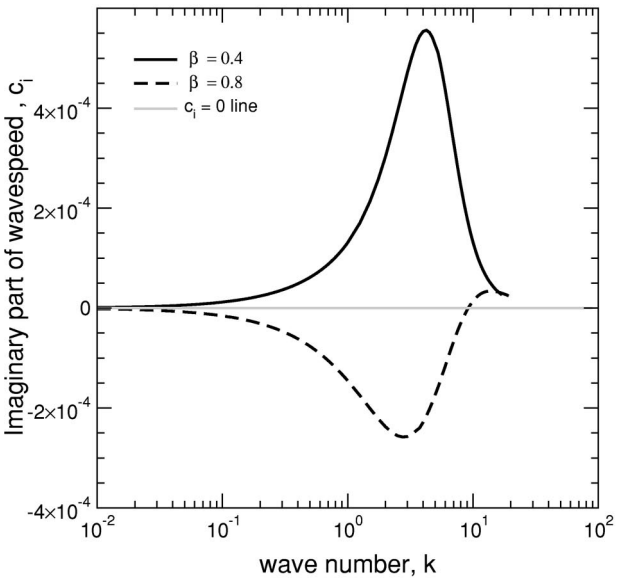

(b) c_i vs. k

FIG. 2. Mode 1 instability in rigid channels: Variation of the real and imaginary parts of the wavespeed c with the wavenumber k for two layer Newtonian Couette flow in rigid channels ($\Gamma=0$). Data for $\mu_r=0.5$, Re=1, and interfacial tension $\Sigma=0$.

formable solid layer. They showed that the interface between the fluid and the solid layer becomes unstable when the parameter $\Gamma=V\mu/(GR)$ exceeds a critical value, even in the creeping flow limit, i.e., Re=0. The variation of c_i with k for this instability is shown in Fig. 4 for two different values of Γ. This shows that the interfacial instability between the fluid and the solid layer is a *finite wavenumber* instability, and hence is qualitatively different from that of the two-layer instability between two fluids. We refer to this interfacial mode between the fluid and the solid as "mode 2" in the ensuing discussion.

The results of the low k analysis of Sec. III reveal that the solid layer could have a stabilizing or destabilizing effect

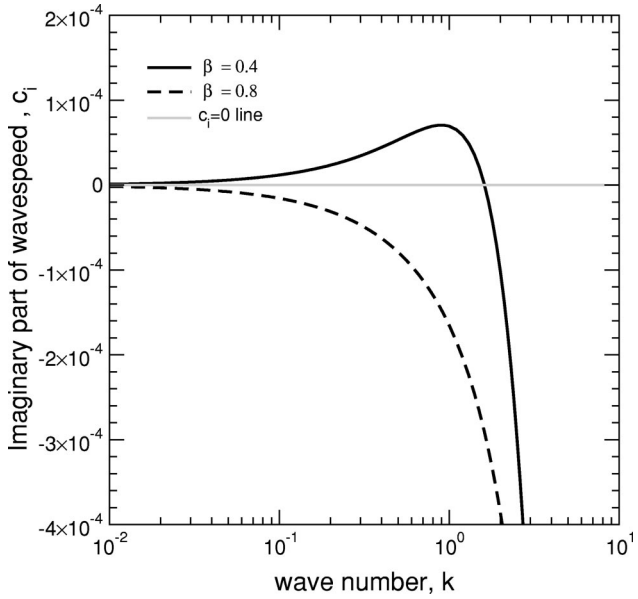

FIG. 3. Mode 1 instability in rigid channels: Effect of nonzero interfacial tension on c_i vs k. Data for $\mu_r=0.5$, Re=1, and $\Sigma=0.01$.

on the two-fluid interfacial mode 1. Three qualitatively distinct cases can be distinguished from these results, and the following issues emerge which will be addressed below through the numerical solution of the stability equations.

(1) Mode 1 is unstable in rigid channels, and the solid layer has a stabilizing effect on mode 1 in the low wavenumber limit: In this case, the question arises whether the predicted stabilization extends to finite k and what is the effect of solid layer on the two-fluid mode (mode 1) at finite k? Also, the interfacial mode between the fluid and the solid (mode 2) becomes unstable at finite k when Γ increases beyond a critical value. A pertinent question, therefore, is: at fixed Re, is there a sufficiently large

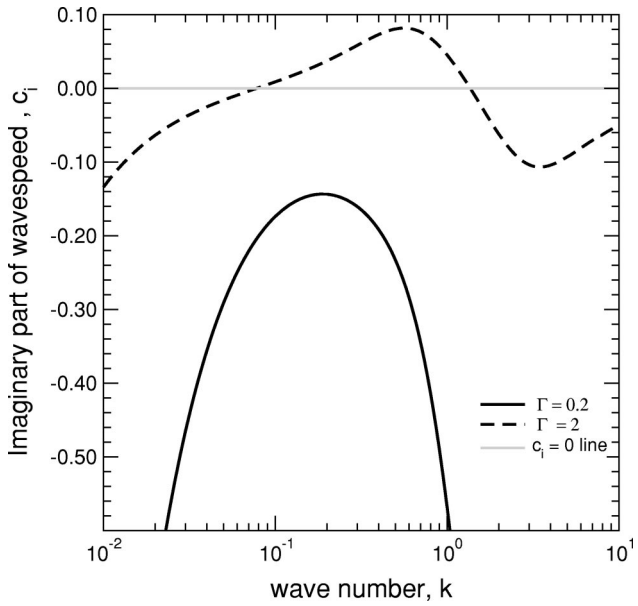

FIG. 4. Mode 2 instability in single layer Couette flow past a deformable solid layer: variation of c_i with k for $H=4$, Re=0, and $\eta_r=0$.

window in the parameter Γ where both modes 1 and 2 are stable? In the limit of low k, the solid-fluid viscosity ratio η_r has no effect on the first correction to the wavespeed $c^{(1)}$, and hence has no effect on the Γ required to stabilize mode 1. However, at finite k, η_r can affect both modes 1 and 2, and this effect will be examined by the above numerical procedure.

(2) Mode 1 is stable in rigid channels, and the solid layer has a destabilizing effect in the low wavenumber limit: Here, the effect of the solid layer on finite k perturbations of mode 1, and the effect of increasing Γ on mode 2 need to be investigated.

(3) Mode 1 is stable in rigid channels and the solid has a stabilizing effect on mode 1: In this case, the question arises as to whether the two-fluid interfacial perturbations have any effect on the critical Γ required to destabilize the fluid–solid interfacial mode (mode 2).

There is another possibility wherein mode 1 is unstable in rigid channels, and the solid layer has a destabilizing effect on mode 1. Since the solid layer merely has a destabilizing effect on an already unstable mode 1, we do not discuss this case below.

We first discuss the case where the solid layer has a stabilizing effect on mode 1, when it is unstable in the long-wave limit in the absence of the solid layer. Figures 5(a) and 5(b) show the variation of c_i with k for $\Gamma=0.2$ for both $\Sigma=0$ and $\Sigma=0.05$. Without loss of generality, we set the Reynolds number $\mathrm{Re}=1$ in the following numerical results. When $\mathrm{Re}=0$, the two-fluid interfacial instability is absent, and the only possible instability is the mode 2 instability which has been studied earlier by Kumaran *et al.*[3] and recently by Gkanis and Kumar.[17] This instability will occur when the nondimensional parameter Γ exceeds a critical value. However, we show below that for values of Γ much less than that required to excite the mode 2 instability, it is possible to stabilize the mode 1 instability at finite Re. Figure 5(a) also shows the variation of c_i vs k for the two-layer interfacial mode in rigid channels (i.e., without the solid layer; $\Gamma=0$). For $\Sigma=0$, this interfacial mode is unstable at all k for $\Gamma=0$. For $\Gamma=0.2$, Fig. 5(a) shows that the stabilization due to the solid layer predicted by the low k analysis is indeed carried over to $k\approx 1$. However, for $k>1$, the interfacial mode between the two fluids is unstable, and the values of c_i for $k>1$ are in fact larger than the c_i for the case when $\Gamma=0$. This is further illustrated in Fig. 5(b) where only the $k>1$ region is shown for the same data set as in Fig. 5(a). This shows that at $k>1$, the solid layer in fact has a destabilizing effect on mode 1, and this is over and above the existing two-layer instability in the absence of the solid layer. However, for nonzero interfacial tension $\Sigma=0.05$ in between the two fluids, mode 1 is stabilized completely at all k. This example thus shows that while solid layer deformability has a stabilizing effect for $k\leqslant 1$, it could be destabilizing at higher k, and only the interfacial tension between the two fluids can stabilize the instability at such large k. It is also useful here to estimate the nondimensional interfacial tension $\Sigma=\gamma/(V\mu_b)$ in order to make connection with typical experimental systems. The interfacial tension for viscous liquids is typically about $0.02\ \mathrm{N\,m^{-1}}$, and we use $\rho=10^3\ \mathrm{kg\,m^{-3}}$, $\mu_b=10\ \mathrm{kg\,m^{-1}\,s^{-1}}$. The fluid velocity $V=10^{-2}\ \mathrm{m\,s^{-1}}$ for $\mathrm{Re}=10^{-2}$ and $R=10^{-2}$ m. For these values, the nondimensional parameter $\Sigma=0.2$. Therefore, one may expect Σ to be in the range 10^{-2}–10^{-1}.

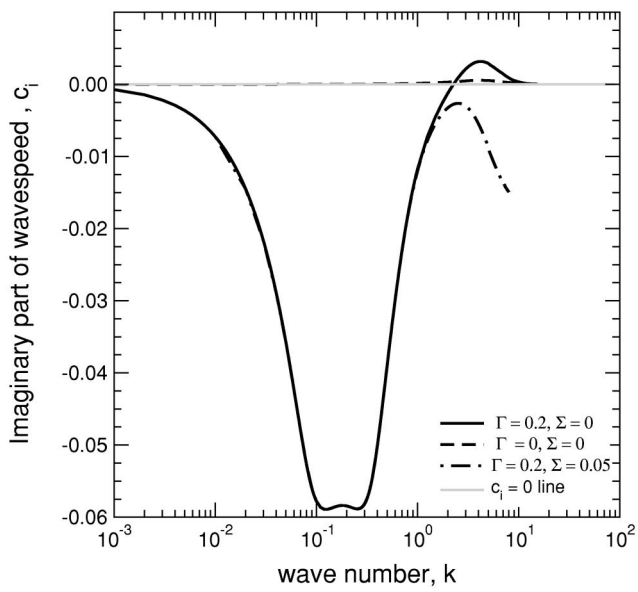

(a) c_i vs. k

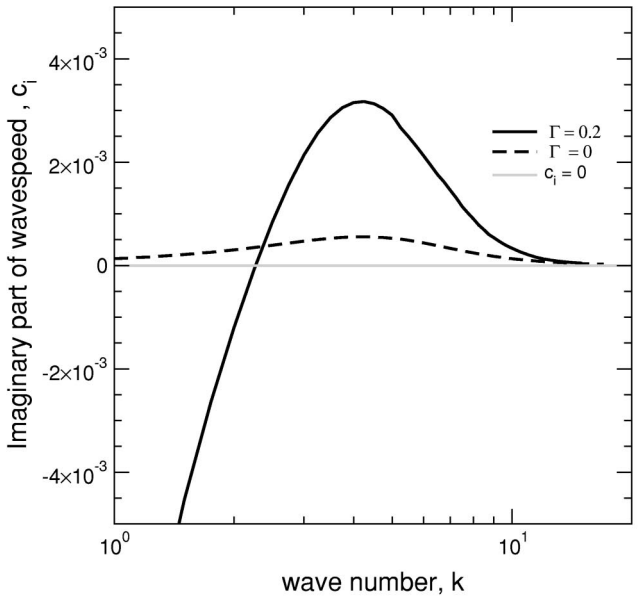

(b) c_i vs. k in the range $k \geq 1$; $\Sigma = 0$

FIG. 5. Effect of solid layer deformability on mode 1: c_i vs k for $\Gamma=0.2$, $\beta=0.4$, $\mu_r=0.5$, $H=4$, $\mathrm{Re}=1$, and $\eta_r=0$.

The variation of c_i vs k for mode 2 (the interfacial mode between fluid B and the solid layer) is shown in Fig. 6(a) for $\Gamma=0.2$, and this shows that the mode 2 instability is not excited for $\Gamma=0.2$. Figure 6(b) shows c_i vs k data for $\Gamma=2$, both for modes 1 and 2, for $\Sigma=0.01$. This indicates that while mode 1 remains stable due to the solid layer, mode 2 becomes unstable at this value of Γ. While the foregoing

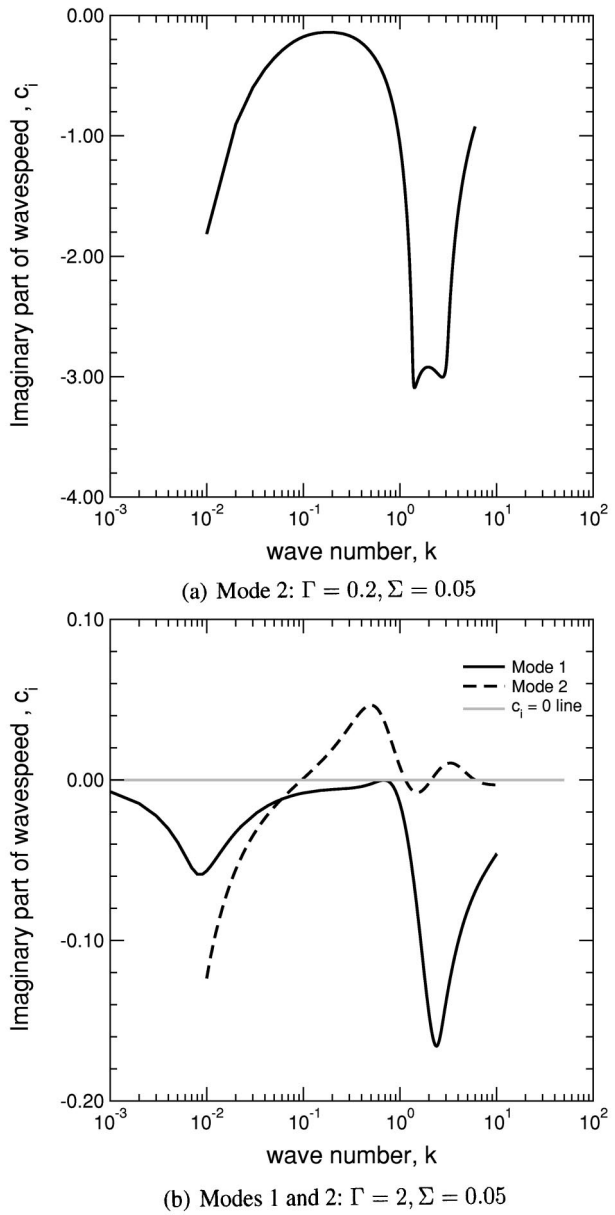

FIG. 6. Effect of solid layer deformability on mode 1 and mode 2: c_i vs k for $\beta=0.4$, $\mu_r=0.5$, $H=4$, Re=1, and $\eta_r=0$.

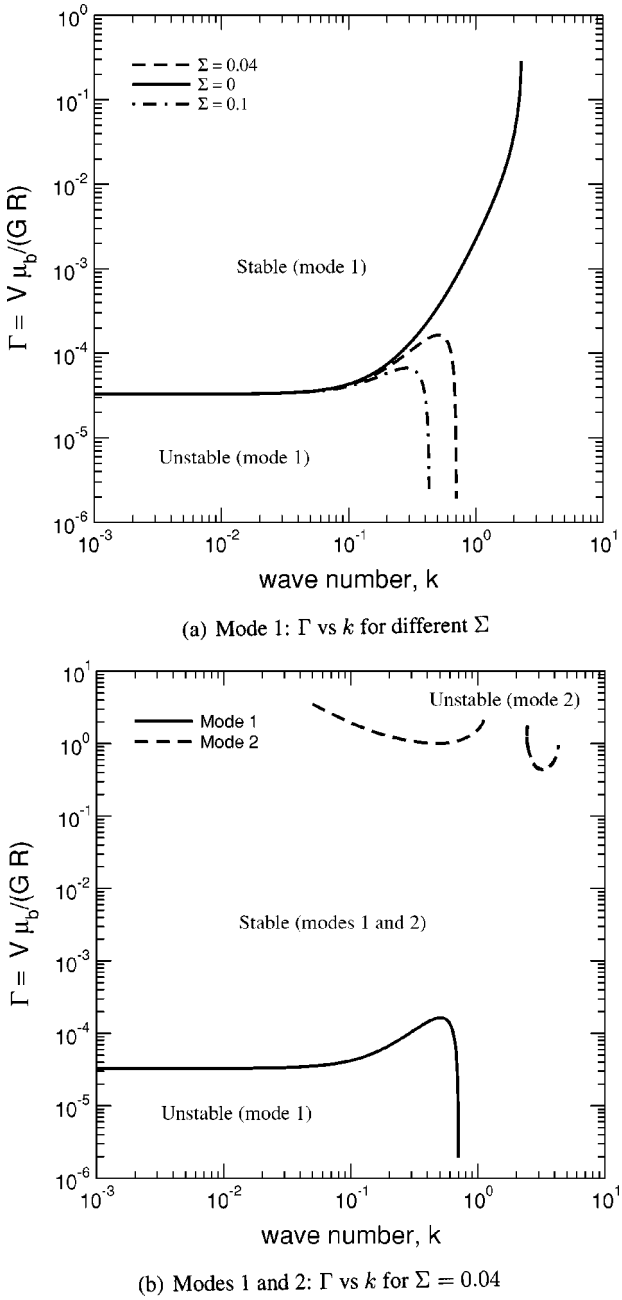

FIG. 7. Neutral stability curves for mode 1 and mode 2: Γ vs k for $\beta=0.4$, $\mu_r=0.5$, $H=4$, Re=1, and $\mu_r=0$.

illustration of stabilization of mode 1 (and destabilization of mode 2) upon increase of Γ was based on c_i vs k curves, it is instructive to construct *neutral stability* curves demarcating stable and unstable regions in the Γ-k plane, for fixed values of Re, μ_r, β, H, η_r, and Σ. Such plots will then allow us to select the parameter Γ (or equivalently, the shear modulus of the solid layer) so that both mode 1 and mode 2 are stable in the three-layer configuration. Figure 7(a) shows the neutral curve for mode 1 for three different values of Σ. There is a transition from unstable to stable perturbations when Γ is increased beyond the neutral stability curve. For $\Sigma=0$, the stable region remains only for $k\approx 1$, while $k>1$ perturbations are always unstable, and this is in agreement with the c_i vs k results shown in Fig. 5(a). For $\Sigma \neq 0$, however, unstable perturbations of mode 1 are confined to $k<1$ in the Γ-k plane, and the flow is stable at all wavenumbers when Γ is greater than a critical value. A useful guide to this critical value is the result from the low wavenumber analysis [Eq. (53)], although at finite k, the Γ required for stabilization is somewhat larger than that predicted in the low wavenumber analysis. The neutral curves for both the modes are provided (for $\Sigma=0.01$) in Fig. 7(b). When Γ is increased beyond the mode 1 neutral curve, there is a transition from unstable to stable perturbations, while when Γ is increased beyond the mode 2 neutral curve, there is a transition from stable to unstable perturbations. Two neutral curves appear for mode 2, corresponding to the two peaks in the c_i vs k curve for mode 2 shown in Fig. 6(b) for $\Gamma=2$. As demonstrated in this figure, there is a substantial "window" in the parameter Γ (or, equivalently, the shear modulus of the solid layer) where

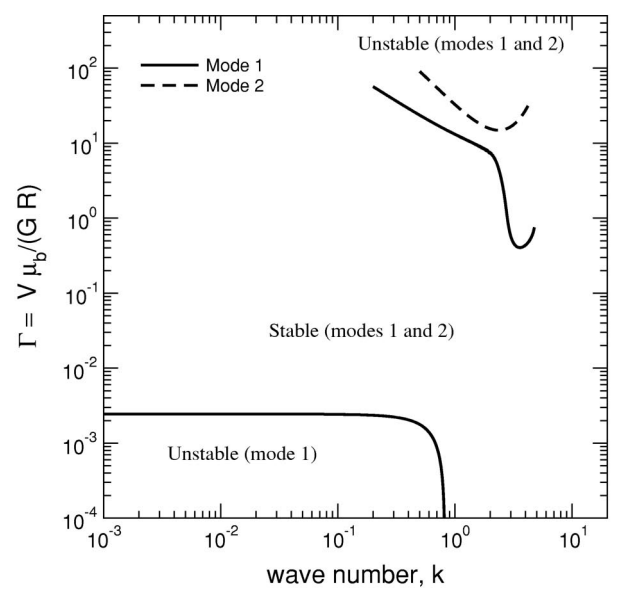

(a) Neutral curve: Γ vs k

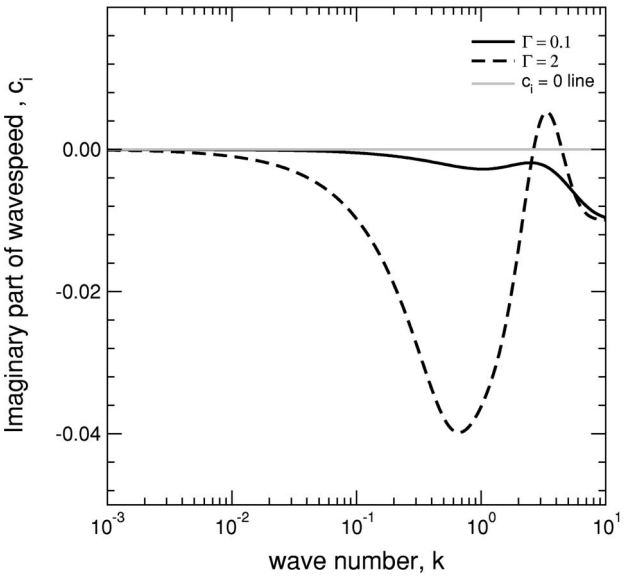

(b) Modes 1 and 2: c_i vs k

FIG. 8. Stabilization of mode 1 by the solid layer: Neutral curve and imaginary part of wavespeed: Data for for $\beta=0.4$, $\mu_r=0.5$, $H=0.5$, Re$=1$, $\Sigma=0.03$, and $\eta_r=0$.

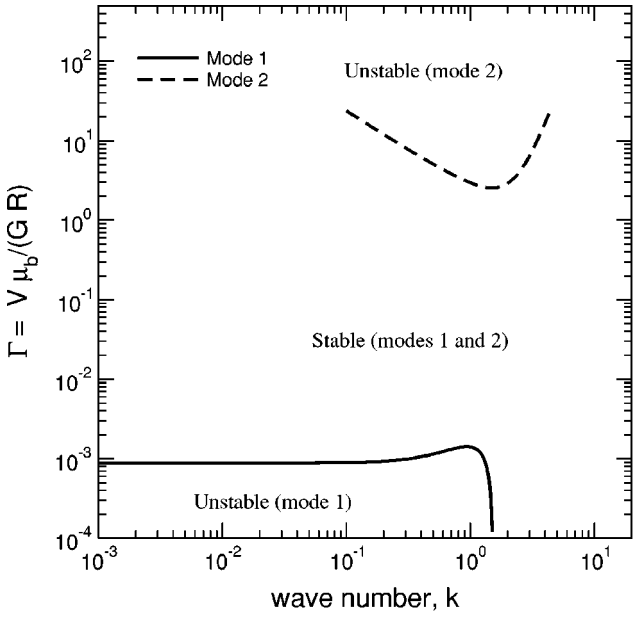

(a) $\beta=0.8, \mu_r=4, \Sigma=0.1, H=1, Re=1, \eta_r=0$

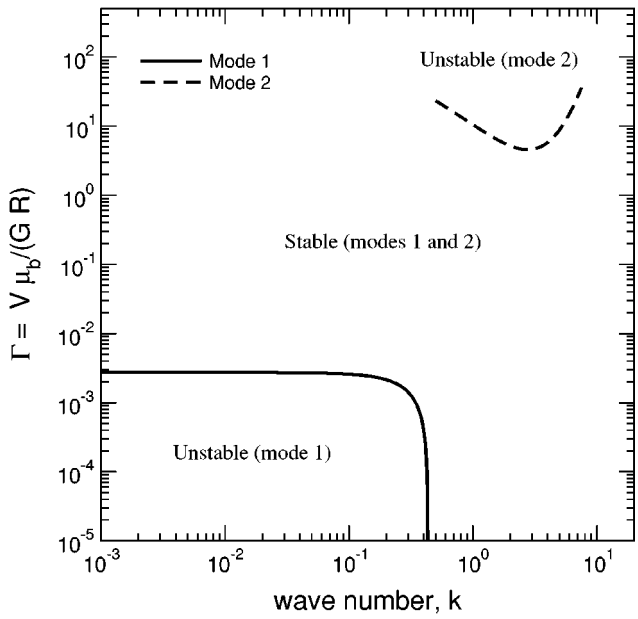

(b) $\beta=0.6, \mu_r=2, \Sigma=0.1, H=0.5, Re=1, \eta_r=0$

FIG. 9. Stabilization of mode 1 by the solid layer: Neutral curve for mode 1 and mode 2 for two different parameter sets.

both the interfacial modes are stabilized. It is useful to illustrate how this translates in terms of dimensional values of shear modulus G. To this end, we consider Fig. 7(b) where Re$=1$ and the region where both the modes are definitely stable ranges from $\Gamma\sim10^{-4}$ to $\Gamma\sim10^{-1}$. Let us consider the velocity independent ratio Re$/\Gamma$: since Re$=1$ in the figure, $\Lambda\equiv \mathrm{Re}/\Gamma=\rho G R^2/\mu_b^2$ ranges from 10^4 to 10. To estimate G, we use $\rho=10^3$ kg m^{-3}, $\mu_b=10$ kg m^{-1} s^{-1}, $R=10^{-2}$ m. Using the mentioned range for Λ, we conclude that G should be in the range 10^7-10^4 Pa in order for both the modes to be stable.

Figure 8(a) shows the neutral curve for the same data set as in Fig. 7(b) but for $H=0.5$. This again shows that mode 1 is stabilized when Γ is greater than a critical value, and since $\Sigma\neq0$, the unstable region is confined to finite k, and high k modes are stable. However, when Γ is increased beyond a certain higher value, the interfacial mode 1 is again destabilized, but only at high k. This is demonstrated in terms of c_i vs k in Fig. 8(b). This figure shows that while mode 1 is stable at all k for $\Gamma=0.1$, it is unstable to perturbations with $k\approx2$ when $\Gamma=2$. In other words, increasing Γ above a critical value has a destabilizing effect on finite k perturbations. However, the presence of sufficiently high interfacial Σ will stabilize these unstable perturbations. Figures 9(a) and 9(b) again demonstrate for different parameter sets that there is a wide window of the parameter Γ in which both the interfa-

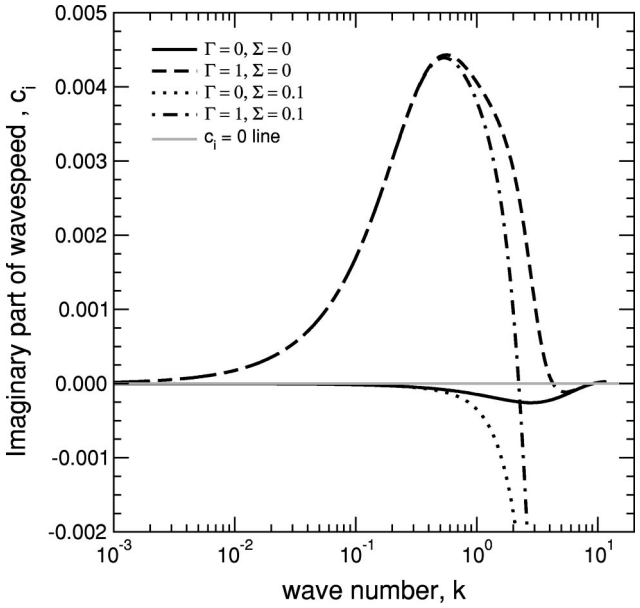

FIG. 10. Destabilization of mode 1 by the solid layer ($\Gamma \neq 0$) when it is stable in the long-wave limit in rigid walled channels. c_i vs k for $\beta=0.8$, $\mu_r=0.5$, Re$=1$, $H=0.5$. Also shown is the curve for two-layer flow in rigid channels, i.e., when $\Gamma=0$.

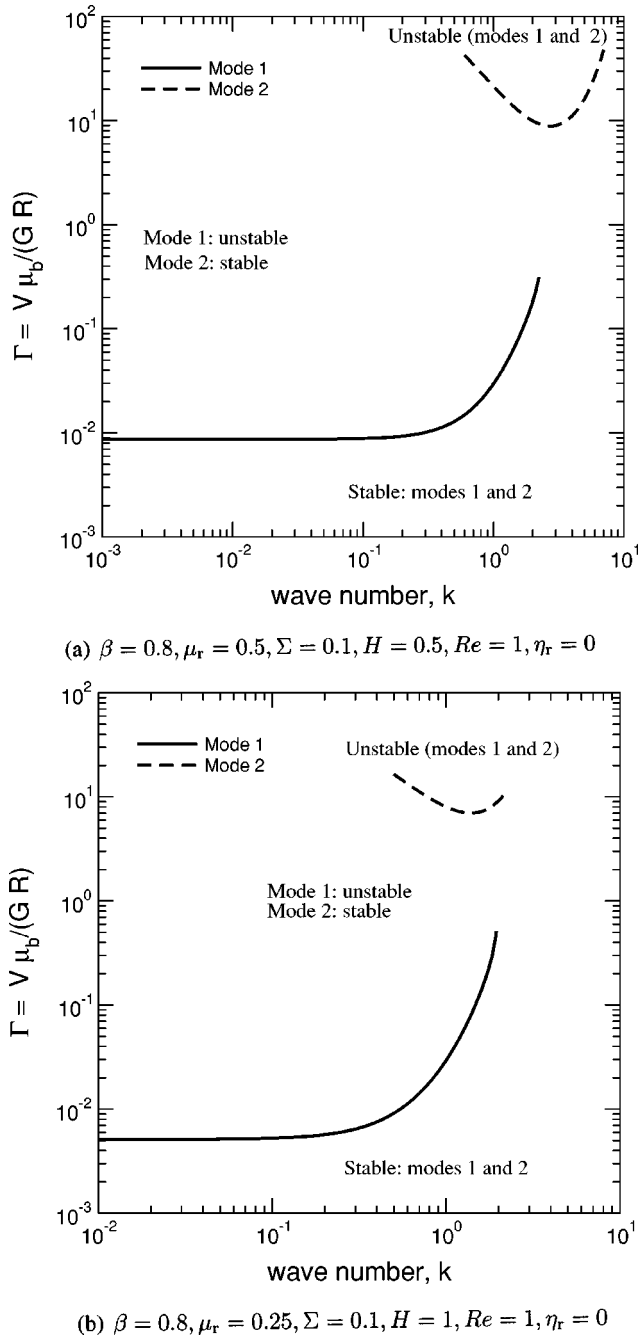

FIG. 11. Destabilization of mode 1 by the solid layer: Neutral curve for mode 1 and mode 2 for two different parameter sets.

cial modes are stable at all k, and so by appropriately tuning the shear modulus of the solid layer, it must be possible to achieve complete stabilization.

We next turn to the case when the solid layer has a destabilizing effect for low k on mode 1, when it is stable in rigid walled channels. Figure 10 shows c_i vs k for such a case, both for $\Sigma=0$ and $\Sigma\neq 0$. Also shown in this figure is the variation of c_i vs k for $\Gamma=0$, i.e., the case of two-layer flow in a rigid walled channel. This figure shows that the predicted destabilization of mode 1 for $\Gamma\neq 0$ extends to finite and large k. For $k\gg 1$, the interfacial mode becomes unstable even in a rigid channel when $\Sigma=0$ (similar to the short-wave instability of Hooper and Boyd[15]), and both the curves for $\Gamma=0$ and $\Gamma=1$ merge for $k>10$, as one would expect the effect of solid layer to diminish for short wavelength perturbations. For nonzero interfacial tension Σ, however, the short-wave instability is absent, and only low and finite wavenumber modes are destabilized. Figures 11(a) and 11(b) demonstrate the destabilization of mode 1 by the solid layer through neutral stability curves in the Γ-k plane. Here, there is a transition from stable to unstable modes when both the neutral curves (corresponding to mode 1 and mode 2) are crossed by increasing Γ.

The low k asymptotic results also revealed that the stabilization or destabilization of mode 1 in the low k limit depends on H (see, for example, the entry for $\beta=0.6$ in Table III). This is further illustrated in terms of c_i vs k in Fig. 12. Also shown here is the variation of c_i vs k for $\Gamma=0$, the case of two-layer flow in a rigid walled channel. For $\Gamma=0.1$, and $H=3$, mode 1 is always stable at all k, while for $H=10$, it is unstable in the $k\rightarrow 0$ limit, in agreement with the low k asymptotic results. Interestingly, when $H=3$, if Γ is increased further to 1, then mode 1 becomes unstable at *finite* k, which of course could not have been anticipated from the low k results. These data thus demonstrate that by varying the parameters characterizing the solid layer, Γ and H, it is possible to manipulate the interfacial mode between the two fluids.

We now turn to the case when mode 1 is stable in rigid channels, and the solid layer also has a stabilizing effect in the longwave limit: in this case, it is of interest to determine the effect of the fluid–fluid interfacial perturbations on the interfacial mode between fluid B and the solid (mode 2). This is shown in Figs. 13(a) and 13(b). In Fig. 13(a), $\beta=0.4$ and $\mu_r\geqslant 1$, i.e., the less viscous fluid is in between the more viscous fluid and the solid, and as μ_r is increased from 1, the critical Γ required for instability decreases. This can be un-

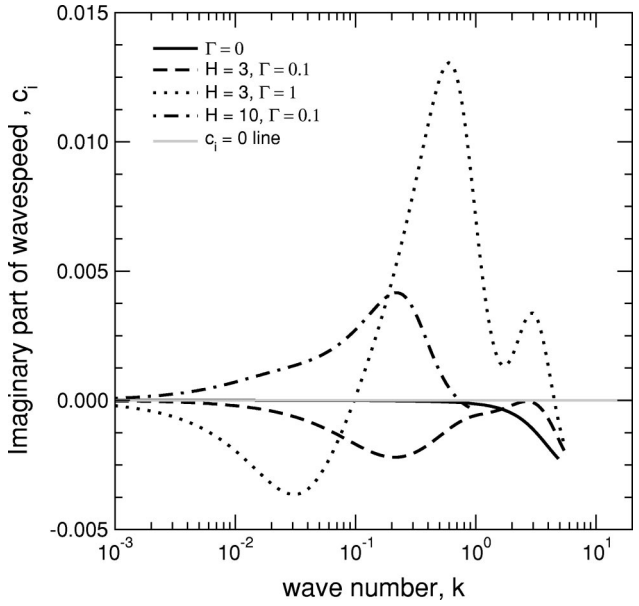

FIG. 12. Effect of H on stabilization/destabilization of mode 1: Data for $\beta=0.6$, $\Sigma=0.01$, $\mu_r=0.5$, Re=1, and $\eta_r=0$.

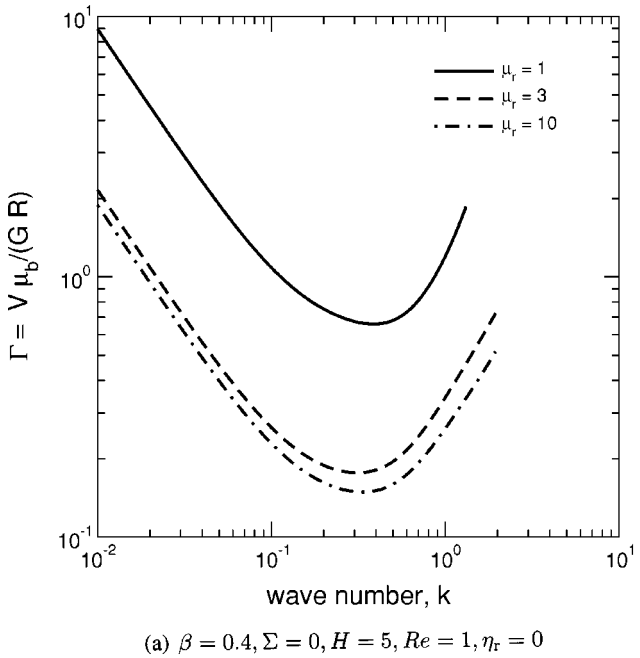

(a) $\beta = 0.4, \Sigma = 0, H = 5, Re = 1, \eta_r = 0$

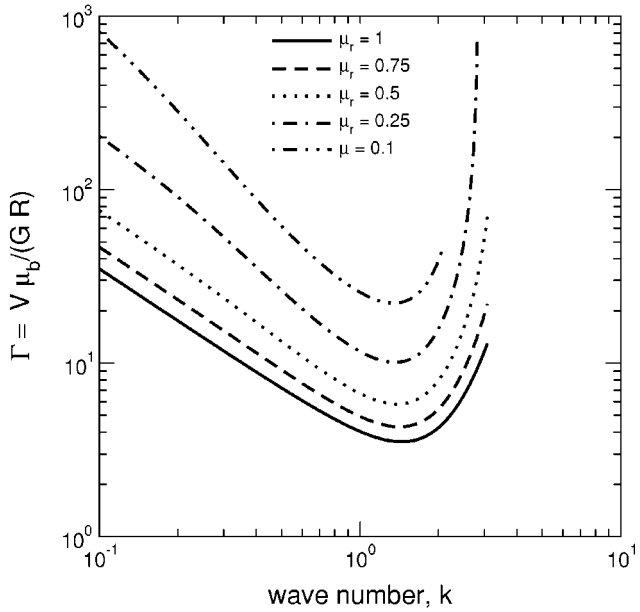

(b) $\beta = 0.6, \Sigma = 0.05, H = 1, Re = 0, \eta_r = 0$

FIG. 13. Effect of μ_r on mode 2 neutral curve, when mode 1 is stable.

derstood by noting that the destabilizing term for the mode 2 instability in the tangential velocity condition between the fluid B and the solid layer (21), $d_z \overline{v_x^b}|_{z=0}$ is proportional to $\mu_r/[1+\beta(\mu_r-1)]$, which increases with an increase in μ_r. Consequently, the Γ required to destabilize mode 2 decreases with increase in μ_r. In Fig. 13(b), $\beta=0.6$ and $\mu_r \leqslant 1$, i.e., the more viscous fluid is in between the less viscous fluid and the solid layer. Here, a decrease in μ_r has a stabilizing effect, as the critical Γ required for the mode 2 instability increases with decrease in μ_r. This can again be understood by observing that the gradient of the base flow in the solid $\mu_r/[1+\beta(\mu_r-1)]$ decreases with a decrease in μ_r, and thus the Γ required for the instability increases with decrease in μ_r.

All the results thus far are for purely elastic solid layers with $\eta_r=0$. Figure 14 shows the effect of nonzero η_r on c_i vs k curves for both mode 1 and mode 2 for the same configuration as in Fig. 6(b). Also shown for comparison are the curves with $\eta_r=0$. This clearly shows that η_r has stabilizing effect on mode 2, and this suggests that nonzero η_r can be utilized to increase the critical Γ required to destabilize the mode 2 perturbations. Figures 15(a) and 15(b) show the neutral curves for both $\eta_r \neq 0$ and $\eta_r=0$ for two different parameter sets. Increase in η_r has negligible effect on the mode 1 neutral curve, but it has a stabilizing effect on the mode 2 neutral curve. In fact, in Fig. 15(a), for $\eta_r=0$ there are two neutral curves for mode 2, but upon increasing η_r to 5, the second neutral curve disappears, indicating that nonzero η_r has stabilized these high k unstable perturbations. A similar trend is found in Fig. 15(b), where the increase in η_r increases the critical Γ required to render mode 2 unstable. This suggests that all the three parameters characterizing the solid layer, viz., Γ (shear modulus), η_r (solid layer viscosity), and H (thickness) can be used to stabilize both mode 1 and mode 2 instabilities in the present three-layer configuration.

Before closing, it is appropriate here to remark on the validity of the use of a simple linear viscoelastic model for the solid layer in this study. The nondimensional base state strain in the solid layer is proportional to Γ [see Eq. (10)] and strictly speaking, the applicability of the linear solid model is valid only when $\Gamma \ll 1$. The earlier study of Gkanis and Kumar[17] which used the neo-Hookean model for the solid has shown, however, that in practice the predictions of the linear solid model remains accurate for $\Gamma \sim 1$, when $H \geqslant 2$ for the interfacial mode between the fluid and the solid layer. Our results for the stabilization of the two-fluid interfacial mode (mode 1) shows that $\Gamma \sim 10^{-3}$ for achieving this effect. Therefore, the present predictions for stabilization and destabilization of mode 1 are expected to be accurate despite the use of a linear solid model, since the Γ required to realize these effects is very small compared to unity. However, the

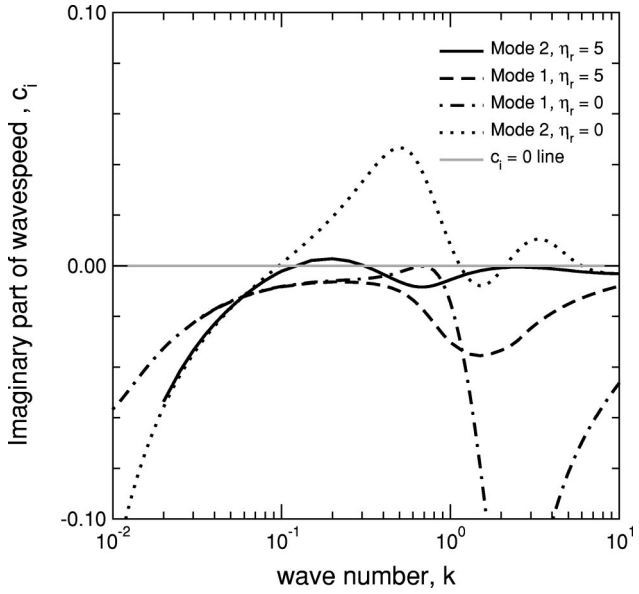

FIG. 14. Effect of η_r on mode 1 and mode 2: c_i vs k for $\Gamma=2$, $\Sigma=0.01$, $\beta=0.4$, $\mu_r=0.5$, Re=1, and $H=4$.

use of a more complex constitutive relation for the solid layer will have some effect on mode 2 neutral curves, and the linear model is expected to be accurate for only $H \geqslant 2$. It must be mentioned that in applications where one might use a soft solid layer to stabilize the two-fluid interfacial instability, it might be advantageous to use solid layers with smaller thickness with $H \leqslant 1$. In such cases of small solid layer thickness, the predictions of the linear solid model for mode 2 must become inaccurate, and it is necessary to use a nonlinear solid model, similar to Gkanis and Kumar.[17]

V. CONCLUSION

In conclusion, our study concerning the stability of the three-layer configuration consisting of two Newtonian fluids undergoing plane Couette flow past a deformable solid layer shows that the solid layer has a profound effect on the interfacial mode due to viscosity stratification between the two fluids (mode 1). Our low wavenumber asymptotic analysis shows that the effect of the solid layer appears at the same order $[O(k)]$ as the destabilizing effect due to fluid inertia in the asymptotic expansion for the complex wavespeed c. Both these contributions could be stabilizing or destabilizing, depending on the fluid viscosity ratio μ_r, relative thickness of the fluid layers β, and the parameters characterizing the solid layer (Γ, H). When the two fluids are arranged so that they undergo a low k instability in rigid channels due to viscosity stratification ($\beta<0.5$, $\mu_r<1$ or $\beta>0.5$, $\mu_r>1$), the solid layer invariably has a stabilizing effect on mode 1. When the two fluids are arranged such that the two-fluid interfacial mode is stable ($\beta>0.5$, $\mu_r<1$ or $\beta<0.5$, $\mu_r>1$), the solid layer could have both destabilizing and stabilizing effects, depending on its thickness. Unlike the case of two-layer flow in rigid channels (where the fluid placement next to the moving or stationary wall has no effect), the low k asymptotic results show in certain cases that the stabilizing or destabilizing effect of the solid layer depends crucially on the placement of the two fluid layers with respect to the solid layer. The nondimensional parameter Γ required achieve this stabilization or destabilization of mode 1 is typically very small compared to unity in the limit of low k. When $\Gamma \sim O(1)$, the interfacial mode between fluid B and the solid layer becomes unstable only at finite wavenumbers, and hence remains stable as $k \to 0$. The results of the low wavenumber asymptotic analysis were continued to finite and higher values of k using a numerical solution of the governing stability equations in the three layers. This shows that while the predicted stabilization due to the solid layer at low k usually extends to finite k, for some configurations, the solid layer could have a destabilizing effect on mode 1 for $k \sim O(1)$. At

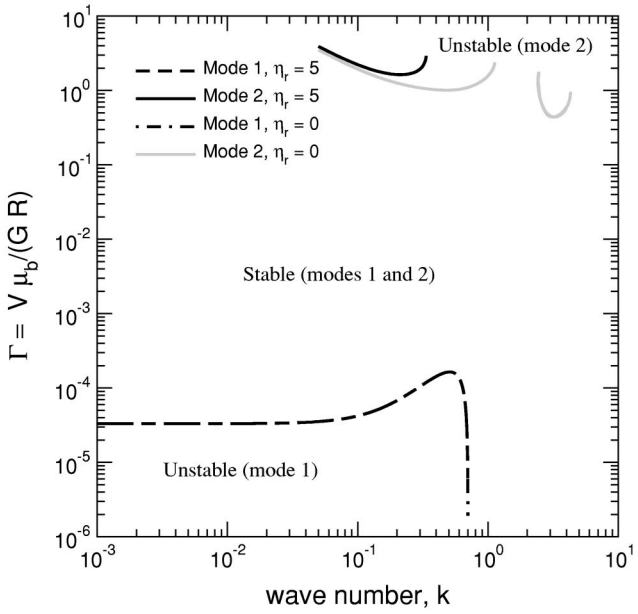

(a) $\beta = 0.4, \mu_r = 0.5, \Sigma = 0.04, H = 4, Re = 1$

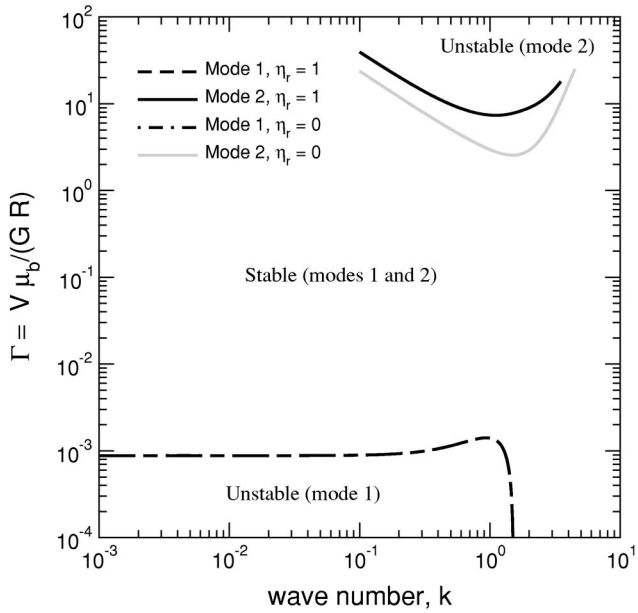

(b) $\beta = 0.8, \mu_r = 4, \Sigma = 0.1, H = 1, Re = 1$

FIG. 15. Effect of nonzero η_r on mode 1 and mode 2 neutral curves.

large k, the solid layer does not have any effect on the interfacial mode between the two fluids, as the perturbations are localized at the two fluid interface for short wavelengths. These finite and short wavelength unstable perturbations can be stabilized only by the presence of a nonzero interfacial tension between the two fluids. At finite k, the interfacial mode between fluid B and the solid layer could become unstable when Γ increases beyond a certain critical value. Neutral stability curves in the Γ-k plane were computed for both the modes, and it was demonstrated that there exists a wide window in the parameter Γ (characterizing the shear modulus of the solid layer) where both the interfacial modes remain stable for all k (for nonzero values of interfacial tension between the fluids). It was shown that all the three parameters characterizing the solid layer, viz., Γ (shear modulus), η_r (solid layer viscosity), and H (thickness) can be tuned to manipulate the two interfacial modes, in order to achieve complete stabilization of the two modes for a given top plate velocity V that drives the Couette flow. It was further demonstrated using typical estimates of the various parameters that the present predictions can be realized in experiments involving two-layer flow of very viscous fluids past soft elastomeric solid layers.

[1] M. A. Unger, H.-P. Chou, T. Thorsen, A. Scherer, and S. R. Quake, "Monolithic and microfabricated valves and pumps by multilayer soft lithography," Science **288**, 113 (2000).
[2] A. Groisman and S. R. Quake, "A microfluidic rectifier: Anisotripic flow resistance at low Reynolds number," Phys. Rev. Lett. **92**, 094501 (2004).
[3] V. Kumaran, G. H. Fredrickson, and P. Pincus, "Flow induced instability of the interface between a fluid and a gel at low Reynolds number," J. Phys. II **4**, 893 (1994).
[4] V. Kumaran and R. Muralikrishnan, "Spontaneous growth of fluctuations in the viscous flow of a fluid past a soft interface," Phys. Rev. Lett. **84**, 3310 (2000).
[5] R. Muralikrishnan and V. Kumaran, "Experimental study of the instability of viscous flow past a flexible surface," Phys. Fluids **14**, 775 (2002).
[6] V. Kumaran, "Stability of fluid flow through a flexible tube at intermediate Reynolds number," J. Fluid Mech. **357**, 123 (1998).
[7] V. Shankar and V. Kumaran, "Stability of non-parabolic flow in a flexible tube," J. Fluid Mech. **395**, 211 (1999).
[8] V. Shankar and V. Kumaran, "Stability of fluid flow in a flexible tube to non-axisymmetric disturbances," J. Fluid Mech. **408**, 291 (2000).
[9] V. Shankar and V. Kumaran, "Stability of wall modes in fluid flow past a flexible surface," Phys. Fluids **14**, 2324 (2002).
[10] C. S. Yih, "Instability due to viscosity stratification," J. Fluid Mech. **27**, 337 (1967).
[11] D. Joseph and Y. Renardy, *Fundamentals of Two-Fluid Dynamics: Part 1, Mathematical Theory and Applications* (Springer, New York, 1993).
[12] M. Gad-el hak, in *IUTAM Symposium on Flow Past Highly Compliant Boundaries and in Collapsible Tubes*, edited by P. W. Carpenter and T. J. Pedley (Kluwer Academic, Dordrecht, 2003), Chap. 9, pp. 191–229.
[13] Y. Renardy, "Stability of the interface in two-layer Couette flow of upper convected Maxwell liquids," J. Non-Newtonian Fluid Mech. **28**, 99 (1988).
[14] K. Chen, "Elastic instability of the interface in Couette flow of two viscoelastic liquids," J. Non-Newtonian Fluid Mech. **40**, 261 (1991).
[15] A. P. Hooper and W. G. C. Boyd, "Shear flow instability at the interface between two viscous fluids," J. Fluid Mech. **128**, 507 (1984).
[16] F. Charru and E. J. Hinch, "'Phase diagram' of interfacial instabilities in a two-layer Couette flow and mechanism of the long-wave instability," J. Fluid Mech. **414**, 195 (2000).
[17] V. Gkanis and S. Kumar, "Instability of creeping Couette flow past a neo-Hookean solid," Phys. Fluids **15**, 2864 (2003).
[18] V. Shankar and S. Kumar, "Instability of viscoelastic plane Couette flow past a deformable wall," J. Non-Newtonian Fluid Mech. **116**, 371 (2004).
[19] L. Srivatsan and V. Kumaran, "Stability of the interface between a fluid and gel," J. Phys. II **7**, 947 (1997).
[20] C.-H. Li, "Instability of three-layer viscous stratified flow," Phys. Fluids **12**, 2473 (1969).
[21] V. Shankar, "Stability of two-layer viscoelastic plane Couette flow past a deformable solid layer," J. Non-Newtonian Fluid Mech. **117**, 163 (2004).
[22] P. Drazin and W. Reid, *Hydrodynamic Stability* (Cambridge University Press, Cambridge, 1981).